



Combined Electrical Tomography (ERT/IP) Methods and Geoelectrical Parameters to Evaluate Groundwater in Qularaisi Area NW Sulaimani City - Kurdistan Region-IRAQ

Ezzadin N. Baban ¹ , Abdulla K. Amin ² , Kwestan M. Ahmed ³ 

¹, Department of Geology, College of Science, University of Sulaimani, Sulaimani, Iraq.

², Department of Social Sciences, College of Basic Education, University of Sulaimani, Sulaimani, Iraq.

³, Groundwater directorate, Sulaimani, Iraq.

Article information

Received: 12- Aug -2022

Revised: 10- Nov -2022

Accepted: 27- Nov -2022

Available online: 30- June- 2023

Keywords:

Electrical Resistivity Tomography
Geoelectrical Parameters
Pumping Test
Sulaimani
Iraq Kurdistan Region

Correspondence:

Name: Ezzadin N. Baban

Email: ezadinb@yahoo.com

ABSTRACT

Sixteen Electrical Resistivity Tomography (ERT) / Induced polarization (IP) traverses were conducted and correlated with pumping test data to estimate aquifer parameters from surface measurements. The 2-D inversion results from this method showed three main electrical layers, the first surface layer is characterized by a low-resistivity value <30 ohms.m which might be interpreted to silty and sandy clays or associated with the water-saturated bed range of the depth 0-20m. The second layer has higher ranges between 80 to 120 ohm.m with a depth of less than 20 m. and represented the variation of grain size sediment sand, silt, and gravel boulder, it is partially saturated with water. Several high-resistivity value features appear in the central part of most of the sections, at a depth below 20m. The third layer is considered a moderate-resistivity value >50 ohms.m., which reflects a bed of silty marl bed of middle Tanjero Fn., this layer acts as an impermeable layer.

The calculated results of hydraulic parameters show the low range of transmissivity is between 4.99–10.65 m²/day with the low range of hydraulic conductivity between 0.05 to 0.17 m/day. This is due to the presence of clay in the area, especially from the direction of Southwest toward northeastern part of the study area, whereas the increasing values were related to the presence of sand or gravel. The hydraulic parameters showing little variations with the aquifer parameters due to the restriction of the study area (little variation in lithology), and the low of the wells production.

DOI: [10.33899/earth.2023.135144.1024](https://doi.org/10.33899/earth.2023.135144.1024), ©Authors, 2023, College of Science, University of Mosul.

This is an open-access article under the CC BY 4.0 license (<http://creativecommons.org/licenses/by/4.0/>).

استخدام طريقتي التصوير المقطعي الكهربائي (ERT / IP) والمعلومات الجيوكهربائية لتقييم المياه الجوفية في منطقة القليسي شمال غرب مدينة السليمانية- إقليم كردستان - العراق

عزالدين نجم الدين بابان¹ ID، عبد الله كريم أمين² ID، كويستان محمد أحمد³ ID
¹ قسم علوم الأرض، كلية العلوم، جامعة السليمانية، السليمانية، العراق.
² قسم العلوم الاجتماعية، كلية التربية الأساسية، جامعة السليمانية، السليمانية، العراق.
³ مديرية المياه الجوفية، السليمانية، العراق.

المخلص	معلومات الارشفة
تم تنفيذ ستة عشر مسارا للطريقة الكهربائية (ERT / IP) وتم ربطها ببيانات اختبار الضخ لتقدير معاملات الخزان الجوفى فى شمال غرب السليمانية. تراوحت أطوال المسارات من 310 إلى 400 متر وكانت المسافة بين الأقطاب 10 أمتار. تتميز الطبقة الأولى بقيمة مقاومة منخفضة والتي يمكن تفسيرها إلى الطين الغرينى والرمل أو المرتبطة بنطاق الطبقة المشبعة بالمياه من عمق 0 إلى 20 م. بينما الطبقة الثانية لها نطاقات أعلى من 80 إلى 120 أوم بعمق أقل من 20 م. ويمثل تباين حجم رمل الرواسب والطين والحصى ، فهو مشبع جزئياً بالماء. تظهر العديد من ميزات قيمة المقاومة العالية فى الجزء المركزى من معظم الأقسام ، على عمق أقل من 20 متراً. تعتبر الطبقة الثالثة ذات قيمة مقاومة متوسطة والتي تعكس طبقة من طبقة المرل الطينية من تكوين تانجيرو، تعمل هذه الطبقة كطبقة مانعة للتسرب.	تاريخ الاستلام: 12- أغسطس -2022 تاريخ المراجعة: 10- نوفمبر -2022 تاريخ القبول: 27- نوفمبر -2022 تاريخ النشر الإلكتروني: 30- يونيو -2023
تم استخلاص العديد من العلاقات الخاصة بخزان دار زروق الهيدروليكي والتي تظهر اختلافات طفيفة فى المتغيرات الهيدروليكية مع معاملات الخزان الجوفى بسبب محدودية منطقة الدراسة والتباين الطفيف فى الصخر وانخفاض إنتاج البئر. يظهر وجود محتوى الطين بوضوح فى علاقة المسامية بمقاومة الخزان الجوفى لتكوين تانجيرو. علاوة على ذلك ، كانت قياسات IP ناجحة للغاية فى التمييز بين الطين (ذو قابلية الشحن العالية والمقاومة المنخفضة) والماء (قابلية الشحن المنخفضة والمقاومة المنخفضة).	الكلمات المفتاحية: لتصوير المقطعي للمقاومة الكهربائية البارامترات الجيوكهربائية اختبار الضخ السليمانية إقليم كردستان العراق
	المراسلة: الاسم: عزالدين نجم الدين بابان Email: ezadinb@yahoo.com

DOI: 10.33899/earth.2023.135144.1024, ©Authors, 2023, College of Science, University of Mosul.

This is an open-access article under the CC BY 4.0 license (<http://creativecommons.org/licenses/by/4.0/>).

Introduction

Groundwater resources are more important for the public water supply than surface water. Consequently, groundwater is less susceptible to contamination and pollution compared to surface water. However, groundwater covers 5% to 7% of the water supply in Iraq. Several villages, districts, and cities use groundwater as the main source of drinking water and agriculture purpose (Al-Ansari et al., 2014). In Iraqi Kurdistan Region, drilling wells and the extraction of groundwater for agricultural, domestic, farming, and industrial purposes is increasing at an unsustainable rate, indicating the increased demand of water.

Geophysical tools help in locating groundwater in any hydrogeological setup. Many geophysical techniques are commonly applied to groundwater investigations, such as gravity and magnetic methods, which are generally used to map regional aquifers and large-scale basin features, while seismic refraction method has several applications such as oil exploration in addition to mineral and water exploration (Mota, 1954; Haeni, 1988). However, using electrical and electromagnetic methods have the greatest success in groundwater

studies. Geological formation properties that are critical to hydrogeology, such as porosity and permeability of rocks, can be correlated with electrical conductivity (Rani, 2017). In addition, ERI method is considered an important geophysical method that is widely used in groundwater investigation (Aziz, 2012; Karim et al., 2014). Besides, integration between two or more geophysical methods are very successful to reduce the uncertainty caused by a single geophysical method (Gao et al., 2018; Loperte et al., 2016; Samyn et al., 2014). Integration between IP and ERT can remove the uncertainty caused by low values of electrical resistivity as high IP values indicate clay content, whereas low IP values reveal water content (Revil et al., 2017; Johnson et al., 2010).

Several geophysical methods, namely the 2D electrical resistivity imaging method, that becomes now a wide standard exploration tool in many environmental, groundwater, archaeology, and engineering surveys in the world (Dahlin, 1996). The main purpose of the 2D electrical resistivity imaging method is to determine the subsurface resistivity distribution by making measurements on the ground surface (Loke, 1995-2007). The geoelectrical resistivity method is considered the most useful quantitative method for the determination of the depth, thickness, and the boundary of an aquifer (Zohdy, 1969), and the porosity of the aquifer (Jackson, et al., 1978). Thus, IP and ERT techniques for the characterization of aquifer system (Akhtar et al., 2021), whereas IP measurements are very successful to differentiate between clay (with high chargeability and low resistivity) and weathered/fractured rock saturated with water (for low chargeability and low resistivity) (Hasan et al., 2020). Only in very few cases, IP was applied with the purpose of hydrogeophysical modeling (Slater and Sandberg, 2000; Slater and Lesmes, 2002) and also geoelectrical parameters including transmissivity and hydraulic conductivity, as well as the relationships of the parameters with the resistivity, transverse resistivity and electrical conductivity (Amin, 2008). The main aim of this study is to conduct electrical resistivity/IP to investigate groundwater and its hydraulic parameters in the study area. The details of the present study are represented by hydraulic parameters including porosity (ρ), transmissivity (T), and hydraulic conductivity (K), as well as the direction of the groundwater flow. The aquifer parameters will give valuable informations essentially for the management of groundwater resources.

Moreover, we can say that for the application of the electrical resistivity method to groundwater prospecting in the Qularaisi area, a high resolution is usually desired both horizontally and vertically, and is used to map areas of moderately complex geology.

Location of the studied area

The study area is located in the Qularaisi area, NW Sulaimani City, Kurdistan Region, Iraq. Geographically, it lies in the zone of 38S in the UTM coordinates system exactly between 3939966 and 3939634 N, as well as 531804 and 531905E. 3940110 N and 3939765 as well as 532042 and 532142 E. The basin occupies an area estimated to be about 3,391,153 m² (Fig. 1). This site is chosen due to the few geophysical studies in the area and its surrounding, especially the seismic refraction method, for which yet there is no previous study and also the existence of another verification tools such as outcrops, and boreholes data information which are always helpful in data interpreting. In additions, this area is located in the city center close to a place of residence and will eventually be a residential area in the near future leading to increasing demands on water as a result of rapid increase in population. Thus, this shows the importance and effect of geophysical methods in groundwater investigation in this area and without too much costing.

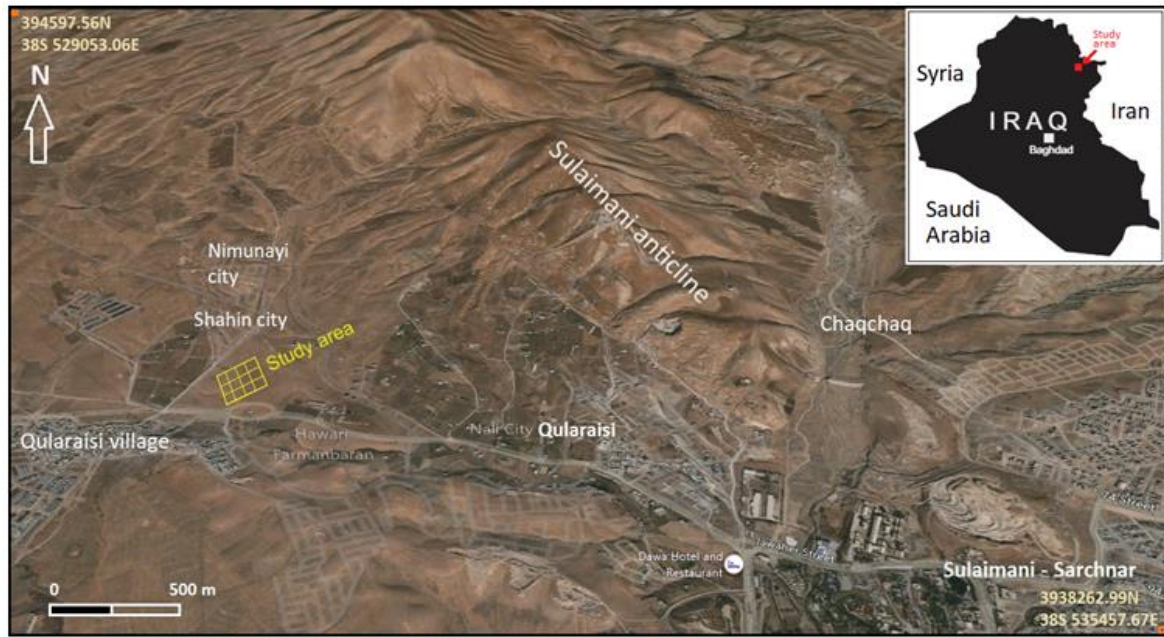


Fig.1. Location map of the study area (Google earth, 2022).

Topography and Geological setting

Topography:

Topographically, the studied area is located in a flat area bounded by abroad mountainous region with Azmur and Goizha mountains covering the northeastern part of the area, whereas the height ranges between 1000 and 1650 m a.s.l., and the plunge of Sulaimani anticline (extension from the big Piramagrun Mountain). Almost 23% of the area is considered a mountainous region which comprises Piramagrun, Azmur-Goizha, Sulaimani anticline, and Baranan homocline, while the central and southern parts of the area, which represent about 77%, are a gently dipping flat terrain.

The Piramagrun anticline is the largest anticline that plunges near Sutka village, the second one is the locally Harmetool anticline (mountain), which is located at the east and southeast of the Piramagrun anticline (Karim et al., 2017). Previously, Harmetool anticline is called Sulaimani anticline (Maala, 2008 and Al-Hakari, 2011). The present study is located in the southeastern limb of Sulaimani anticline which covers half of the surface area of the anticline.

The area is covered by alluvial plain deposits, which are composed of gravels, pebbles, sandy, and sandy silt mixed with clay of the Quaternary period (Stevanovic and Markovic, 2003). The topsoil layer represents an enrichment agricultural plain area, which contains the most essential elements and is bounded by several mountains extending with the same trend of Zagros Mountain belt (NW-SE).

Geologic setting:

The studied area is located in the Nubio-Arabian Platform of a Phanerozoic tectonic unit of the Middle East and belongs to the Unstable Shelf (Buday and Jassim, 1987). There are many stratigraphic units exposed and cropped out in the study area. The age of these units ranges from lower Cretaceous to Quaternary deposits; the oldest rocks cropped out in the crest of anticlines revealing the Balambo Formation that belongs to the Valanginian–Turonian age, whereas the younger units are exposed along with the anticline limbs and in the trough of synclines. The selected stations are located in the Quaternary deposits and Tanjero Formation. Quaternary deposits are composed of a mixture of clay, silt, sand, and gravel with varied thicknesses ranging between 5–15 m. Due to erosion process, the resultant sediments and particles of different sizes around anticlines had been transported to fill the depression and valley areas. In addition, the accumulated rock fragments transported seasonally by stream

floods during heavy rainfall (Ali, 2007). The Tanjero Formation lies under the Quaternary deposits in the study area and represents the thick Upper Cretaceous–Paleogene flysch sequence of the early Zagros Foreland Basin, which developed during the early stage of collision between the Arabian margin and the Tethyan subduction complex to the northeast (Al-Qayim, 1993). The Tanjero clastic Formation comprises two parts. The lower part comprises pelagic marl and occasional beds of argillaceous limestone with siltstone beds, while the upper part comprises silty marl, sandstone, conglomerate, and sandy or silty organic detrital limestone (Sharbazheri and Muhammed, 2009). This is illustrated in Fig. (2).

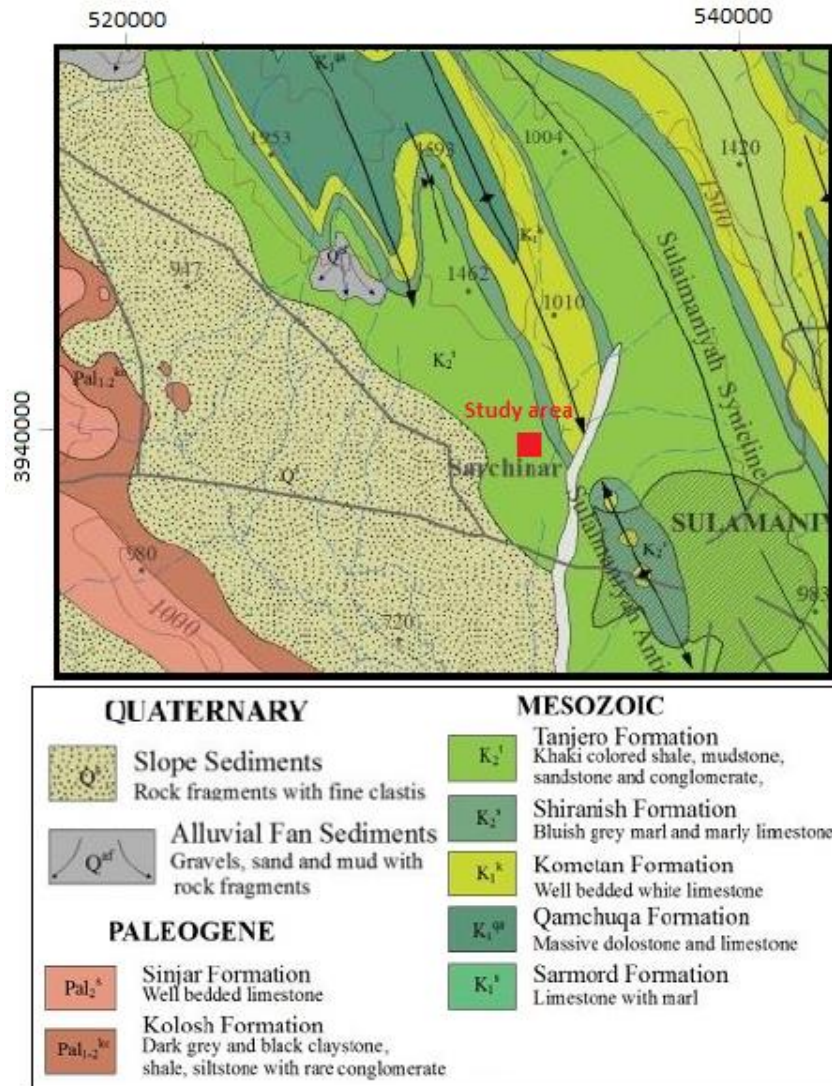


Fig.2. A Geological map of the study area and Sulaimani Governorate (modified from Sissakian and Fouad, 2015).

Hydrology and hydrogeology of the studied area

Hydrologically, the study area is a part of a sub- basin called Sarchnar -Arbat bounded by two main sub-watersheds, one of them is Chaqchaq sub-watershed located in the northeastern part of the studied area, by a distance of about 3 km, whereas the other is Kani-pan sub-watershed, which lies at the southwestern part of the studied area, 9.5 km far from the study area. The confluence of Chaqchaq and Kani-pan streams forms Tanjero River near Kani Goma village. These two streams with tens of smaller ones provide dendritic drainage patterns.

For the current study, the flow net map is constructed based on the data of 27 wells drilled surrounding the area. The information includes the coordinate of the wells, and static water level. The groundwater flow direction is generally from the northeastern towards the

southwestern part of the study area, and this is related to the topography of the area. The flow net map is shown in Fig. (3).

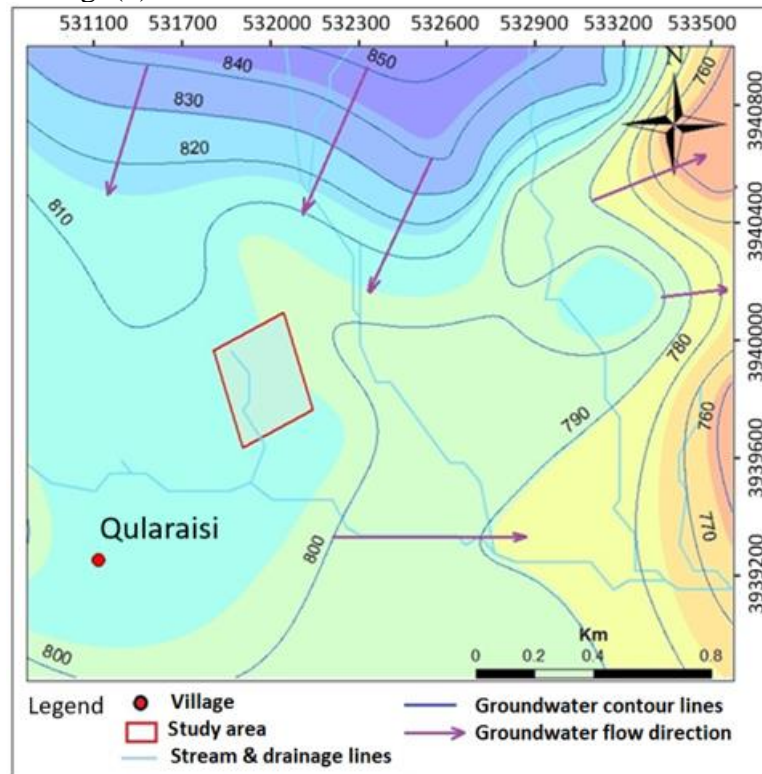


Fig.3. A Flow net map and drainage lines map within the study area done by researcher

From the hydrogeological point of view, the expected groundwater is attributed to subsurface geological conditions, which reflect the presence of shallow to medium aquifer related to recent alluvium and Tanjero Formation.

According to the hydrogeological data and report from the Directorate of Groundwater of Sulaimani, the main productive aquifers in the study area are the Quaternary intergranular aquifer and, in some classifications, the Tanjero Formation is classified as a semiconfined aquifer because of the presence of marl bed in its lower part (Al-Manmi, 2002). The Tanjero Formation is classified as a semiconfined aquifer because of the presence of marl bed in its lower part and of the presence of Shiranish Formation beneath it. According to the data obtained from the Directorate of Groundwater in Sulaimani City, several deep wells exist in the studied area. They include shallow wells in alluvium and deeper in the Tanjero Formation.

About 76 deep wells had been drilled in the area, most of them within the Recent deposits and Tanjero Formation. The yield of these wells' ranges between 6 and 65 gal/min. This different range might be caused by different lithology (Recent/Tanjero Formation) and their depths are between 75 to 200 m. They have static water levels at depths between 10 to 27 m below ground level (BGL) according to the location of the well and seasonal variations. From the total wells drilled near the study area, it is clear that all those drilled in the Tanjero Formation are considered a few successful wells and their yields are comparable due to lithology of the Tanjero Formation consisting of Marl. While recent sediments have few thicknesses in this area.

Fieldwork and data acquisition

Before conducting a geophysical survey for a certain area, the fieldwork must be preceded by conducting a reconnaissance survey of the area based on the target of the study. This survey is comprised of a general overview of the geophysical, geological, geomorphological, and other information such as the presence of wells, geological maps, cross sections, previous geological and geophysical researches.

Depending on the principle of the survey, the site of investigation is located in the Qularaisi quarter near Sulaimani City. Generally, it is a flat agricultural land, whose surface layers are covered by Recent alluvial deposits in addition to the appearance of middle Tanjero Formation at the limb of Sulaimani anticline.

Electrical resistivity tomography (ERT) and induced polarization (IP):

The electrical method is the popular geophysical subsurface imaging techniques applied widely to mineral prospecting, hydrological exploration, environmental investigation, and civil engineering, as well as archaeological mapping. The application of ERT can provide 2D geoelectrical images of subsurface resistivity distribution from which features of contrasting resistivity can be located and characterized where the resistivity changes in the vertical and horizontal directions along the survey line. The main advantage of the ERT survey is to produce a high-resolution image of the subsurface. Because of the sensitivity of resistivity to change in hydrogeological, lithology (e.g., pore fluid composition, water saturation, and clay content) and geological features, an induced polarization (IP) can be used to distinguish between the water and clay layer.

The effective depth of investigation varies between different electrode arrays depending on how the depth of investigation is defined. For the Schlumberger array used in this study, approximately 1/5 current electrodes (AB) are more convenient as a rule of thumb.

The modern computerized instrument ABEM Terrameter LS, manufactured by Sweden Mala is used to conduct field measurements. The ABEM is a standalone system with computer and graphical user interface all built -in, current transmitter, and electrode selector. Figure (4) shows Terrameter LS system in the fieldwork.



Fig.4. Fieldwork imaging survey with Terrameter LS system

Surveys are usually carried out using a large number of electrodes, 41 or more, connected to a multi-core cable, along a straight line that is parallel to the strike direction, and their coordinates can be recorded for each survey line. Cable 1 is connected to cable 2 with a cable joint as well as cable 3 and cable 4 where the cable is closest to the instrument (Fig.5).

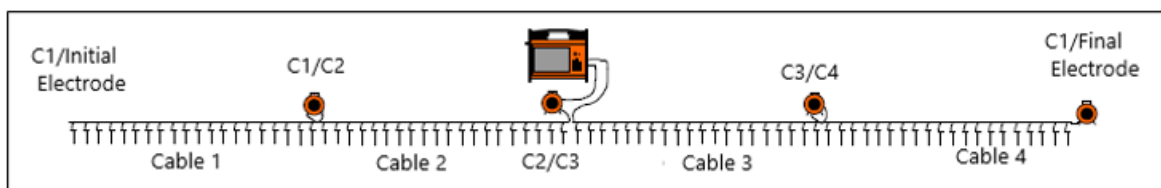


Fig.5. The field arrangement of ABEM Terrameter LS resistivity meter.

In this work, only the application of the 2D electrical resistivity method can provide the hydrogeologic information in an acceptable balance between reliability and cost.

Conducting fieldwork data:

The first stage of the fieldwork is specified for preparing some principal necessities for managing both the 2D fieldwork survey and interpretation. They are digital topographic map, geological map, structural map as well as hydrological and hydrogeological studies on the basin. At the next stage of fieldwork, the ERT data were collected in winter 2021 but four traverse surveys were conducted during 11-17, October, and 4-20 November 2021 in the autumn season, and it took about twelve working days.

Sixteen traverses of electrical resistivity/ induced polarization IP were conducted using the Wenner-Schlumberger array configuration to achieve both vertical and lateral resistivity distributions in the investigated site (Fig. 6).



Fig.6. Base map of the electric traverses survey in the study area (google earth, 2022).

The length of each traverse ranges between 310.0 and 400.0 m, the distance between each traverse was 15-30 m, the electrode-spacing on each traverse was 10 m, and the investigated depth penetration was about 78 m. All the traverses were parallel and oriented with respect to the general trend of the strike (NW-SE) direction, and the coordinates of each traverse were recorded by GPS instrument.

Data processing and interpretation

The 2D resistivity and Induced Polarization (IP) data were processed using the RES2DINV*64 ver. 4.8.10 software. The software directly reads and processes the data and uses a forward and inverse modeling procedure to create a synthetic data set based on measured apparent resistivity. This is an iterative process; a root-mean-square (RMS) error is calculated for each new iteration. Bad data points are progressively removed throughout several iterations until the RMS error is reduced to an acceptable level. The resistivity and induced polarization survey images are presented as a cross-section of the ERT and IP profiles. The data were interpreted by comparing them with the geology of the area and matching with values of electrical resistivity of earth materials. Rock boundaries indicated on the resistivity profiles are certainly based on the available lithological borehole information. The inversion images obtained are based on the 2D inversion high resolution of the field data. The color bar indicates the range of electrical resistivity values in a unit of Ω -meters (Ω s.m). While chargeability (in ms) is measured in the time-domain IP surveys, the color scale is logarithmic and consistent with contour intervals. Cool colors (i.e. blue) represent areas of low resistivity values and warm colors (i.e. red) represent areas of high resistivity values (Sarntim and Arjwech, 2019). The Schlumberger (Winner-Schlumberger) array configuration was used because it is moderately sensitive to the horizontal and vertical structures with an electrode spacing of 10m and traverse's lengths were 400, 380, 360, and 310m. These differences in traverse lengths were due to the restrictedly of the area and the difficulty of spreading the electrodes. All traverses were parallel to the strike of the outcrops (NW - SE). Sixteen 2D ERT Traverses were conducted in the study area.

Interpretation of electrical resistivity tomography traverses:

The first ERT traverse (Res-Tr-1) length is 320m. According to the measured and calculated apparent resistivity pseudosection (Figs. 7 a and b) the area under the traverse consists of different lithological layers; low values at the near surface (blue color) especially at the northwestern of the sections and moderate to high values at the southeastern side and at depths. The inverted section of the traverse (Fig.7c) shows that the resistivity contrast values ranging between 8 to 110 Ω .m. Three layers can be recognized in the section. The first layer is a thin top soil cover layer characterized by a low-resistivity value $< 30 \Omega$.m located mainly at NW of the section and interpreted as a recent deposit (silty and sandy clays), or associated with the partial saturation water bed range of depth 0-10 m. This layer is laid down to a depth of more than 45m at distances between 175 to 255m toward the southeast part making a depression having sharp edges on both sides. This zone is characterized by a low-resistivity value associated with a depression fill with recent sediments mostly composed of clay with weathered marl of the Tanjero Formation. The second layer (feature) is represented by a distinguished and elongated high resistivity value ranging between 80 to 120 Ω .m, located at the SE part of the section and lies at a depth (range of thickness) of 0-20 m which represents variations in grain size sediment sand, silt, and gravel. The third layer is considered a moderate-resistivity value $>50 \Omega$.m reflecting a bed of marl Tanjero Formation. There are several highs and depressions visible on the section at depths of 20m on the NW side and 25m on the SE side. The most obvious one is a high-resistivity value feature (a dyke shape) that lies at the central part of the section, at depth 20 extended downward having sharp edges at both sides, which may be formed due to the weathering of Tanjero Formation. or probably the mesoscopic structure consisting of different lithology (silty marl and silty organic detrital limestone) and/or the presence of a highly fractured marly Limestone interbedded with a layer of sandstone within Tanjero Formation., this might be interpreted as a result of increasing groundwater and it is formed due to that the area was under the different load of pressure and tectonic stress. Tanjero Formation. crops out within the imbricated and high folded zones in Northeastern Iraq (Karim, 2004).

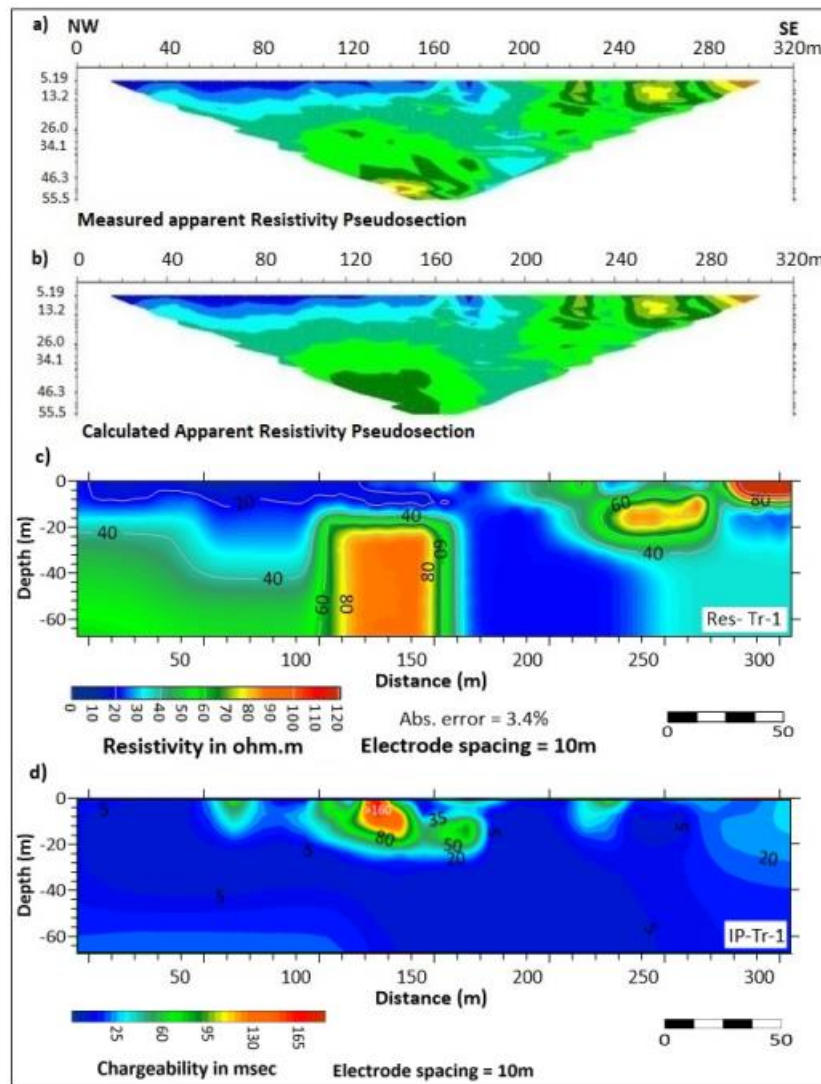


Fig.7. Measured, calculated apparent resistivity pseudosection, ERT inversion model, and IP sections of Tr-1.

Induced polarization survey was performed along the same (RES-Tr-1) traverse using the same electrode spacing and the same number of measurements (Fig.7d). So, IP measurement is used to support the ERT result for integration between clay, and water content whereas high IP values indicate clay content and low IP values reveal water content. The IP result in this section with low resistivity result values in the ERT model (Fig.7) at distance 0-60m low IP and low resistivity indicated water content which at distances 60-170 high IP and low resistivity indicate clay content. As well as the low-resistivity layer laid down to more depth at distances between 175 to 255m is characterized by low IP. So it indicates water content. Also, the same layers and features are distinguished in IP section.

The general geologic setting records that were extracted from the 2D ERT traverses are in quite agreement within these stratigraphic units which are visible on the outcrop closest to the study area by the distance 1500m (Fig. 8). And also, some geological records of the deep wells drilled within this area denote the existence of Tanjero Formation. This is recorded in well No.2, which is located at a distance of approximately 174 m from the traverse-1.

The second and third traverses (Res-Tr-2 and Res-Tr-3) have the same length (320m) as the Res-Tr-1 traverse. The measured and calculated apparent resistivity pseudo sections (Figs. 9 and 10) show the same layers and features that are distinguished in Res-Tr-1 with some differences in their resistivity values.

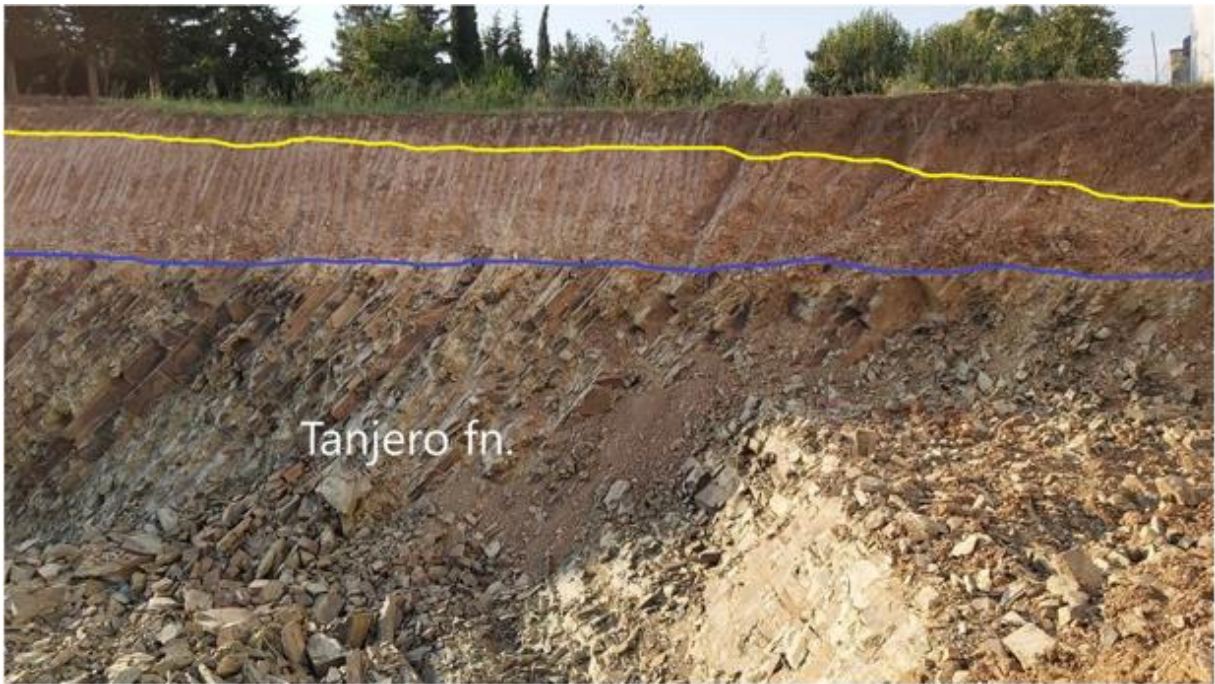


Fig.8. Stratigraphic units exposed on the outcrop at the adjacent site in the study area.

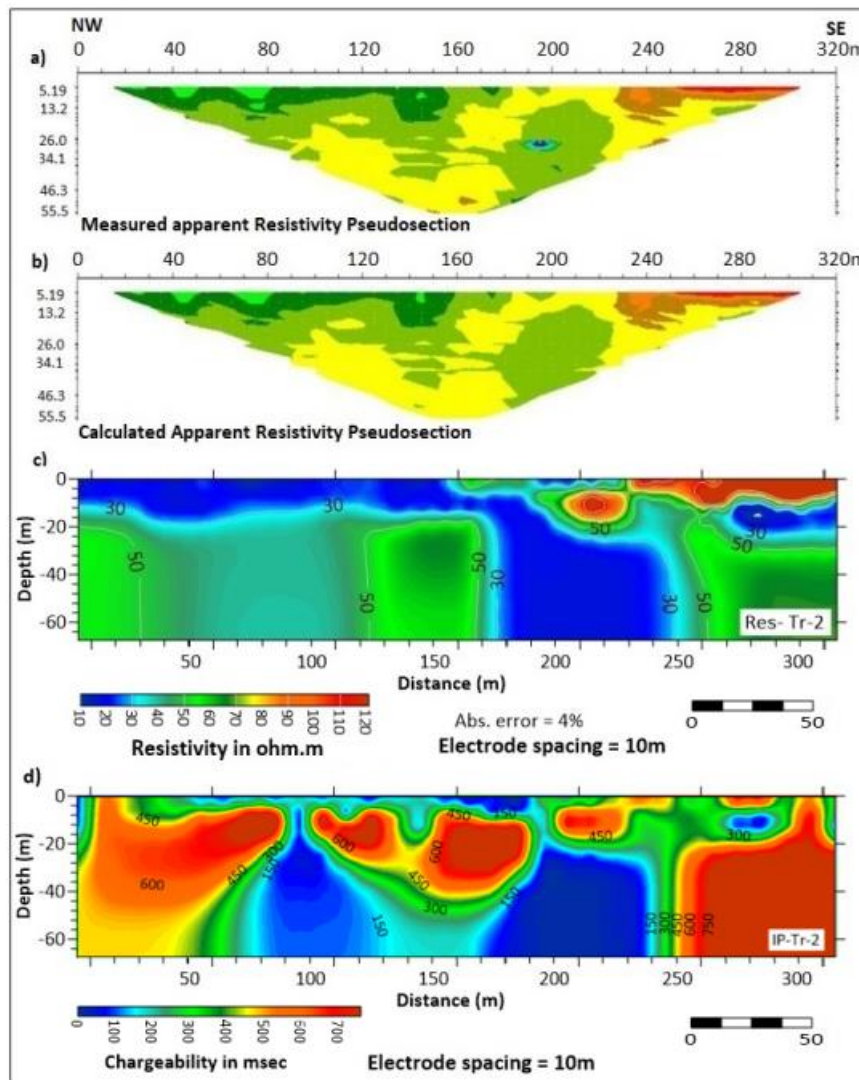


Fig.9. Measured, calculated apparent resistivity pseudosection, ERT inversion model, and IP sections of Tr-2.

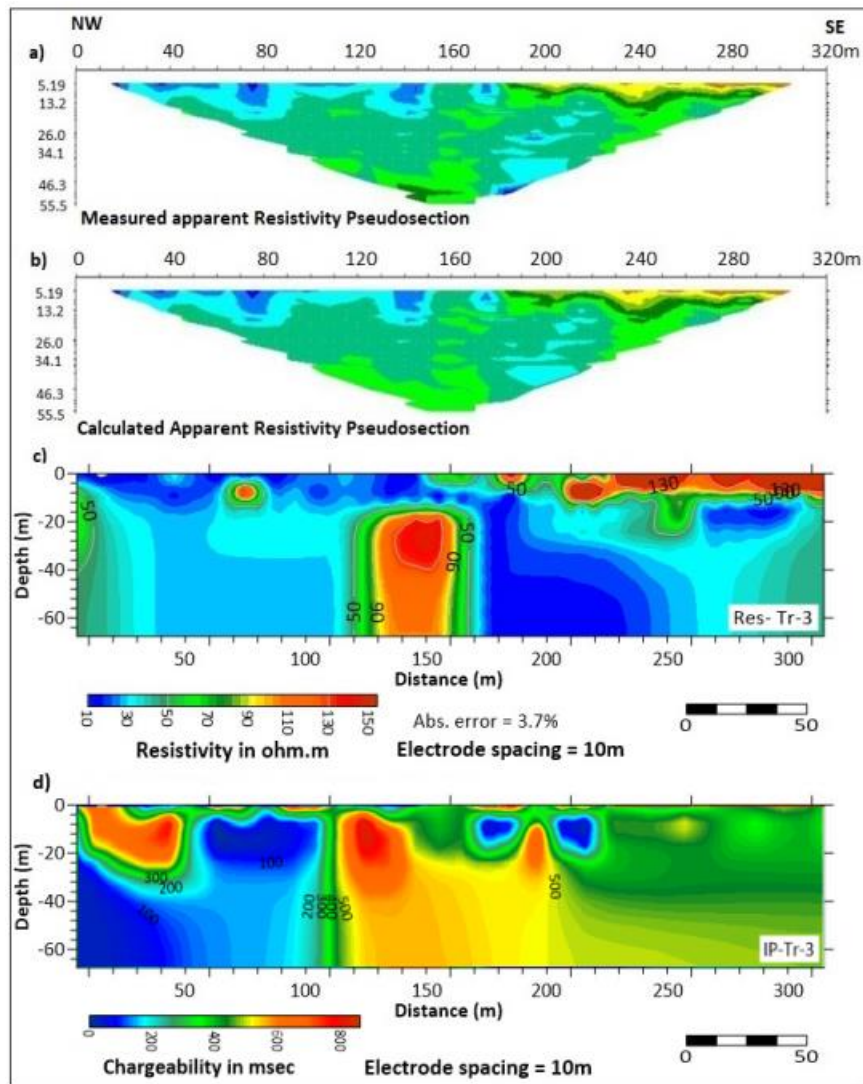


Fig.10. Measured, calculated apparent resistivity pseudosection, ERT inversion model, and IP sections of Tr-3.

Just like the Res-Tr-2, Res-Tr-3, IP was conducted for IP-Tr2 and IP-Tr-3. (Figs. 9d and 10d) show the same layer and feature as that of the result for traverse (IP-Tr-1). At distances between 175 to 255m low resistivity and low IP at a depth more than 10m indicate water content the upper low resistivity layer has high chargeability indicating clay content. Furthermore, at a depth of more than 20m the layer has high resistivity compared to high chargeability indicating hard rocks of Tanjero Formation. Res-Tr-3 has low resistivity value (high IP) generally, it seems indicating clay content. But at left-hand-side, the low resistivity and low chargeability reflect water content and with that in central part of IP section (high IP, high-resistivity value feature) it represents to possibility of fractured marly Limestone of Tanjero Formation.

The Res-Tr-6 traverse has a length of 360m (Fig. 11) and it differs from the above-mentioned traverses. It is characterized by the presence of several low and high resistivity features having different shapes and dimensions. A strip of small and low resistivity features (blue and light blue colors) ranges between 0 and 20 Ω .m visible and spread on both sides of the traverse extended from surface to depths ranging between 5 to 20m which represents the first layer consisting of recent deposit (clay, sand, and silt cycles). The irregular layer (green and light green colors) which lies under the first layer represents the second layer having resistivities ranging between > 20 and $< 40\Omega$.m. This layer mostly reflects the silty marl bed of Tanjero Formation.

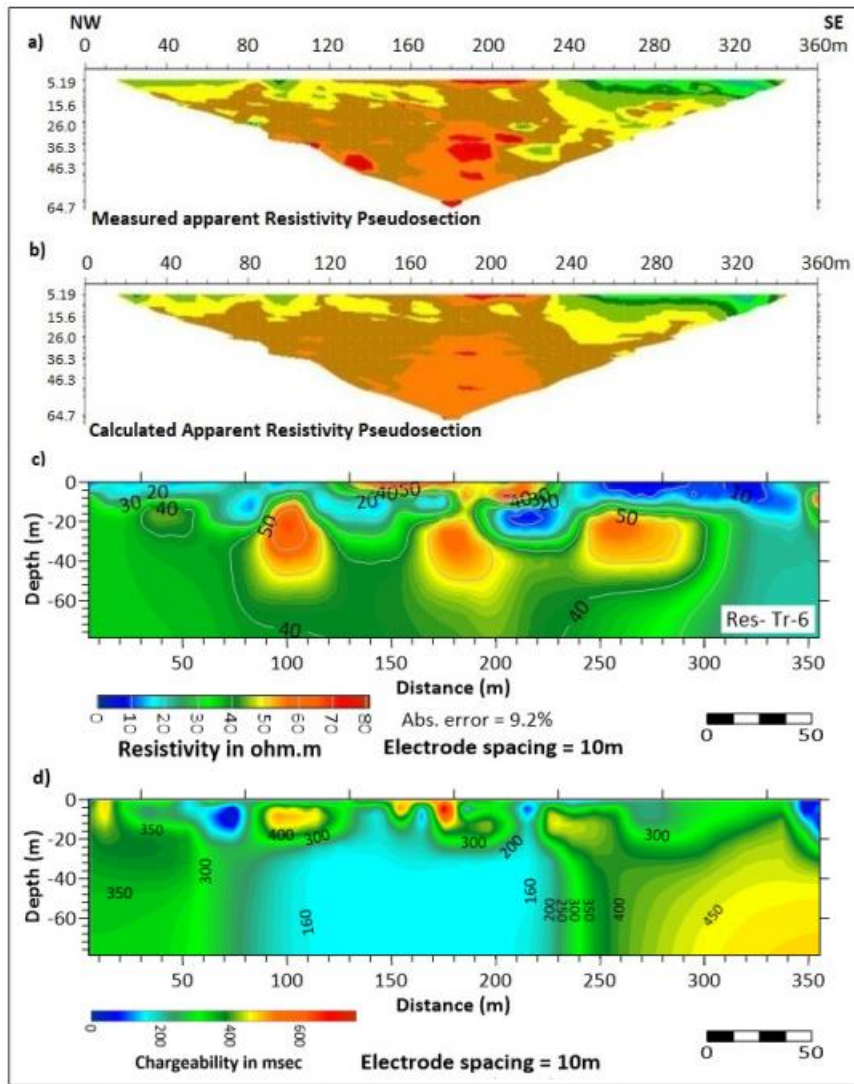


Fig.11. Measured, calculated apparent resistivity pseudosection, ERT inversion model, and IP sections of Tr-6.

Also, there are three semi-circular high resistivity features (orange and red colors) having more than $70 \Omega \cdot m$ lying at distances from 105 to 310m and a depth of 20m and extending downward to a depth of 45m. These high features may be formed due to the highly fractured marly Limestone of Tanjero Formation interbedded with a layer of sandstone or water within Tanjero Formation and they are suitable for drilling exploitable water wells. The top of these features corresponds to the top of the third layer within Tanjero Formation. As well as the IP measurement for these sections was confirmed by the low resistivity same as a pocket (low IP) appeared from the IP sections which are considered by pocket water content as illustrated in Fig. 11d. Also, there are three semi-circular high resistivity features with a low IP indicating fractured rock.

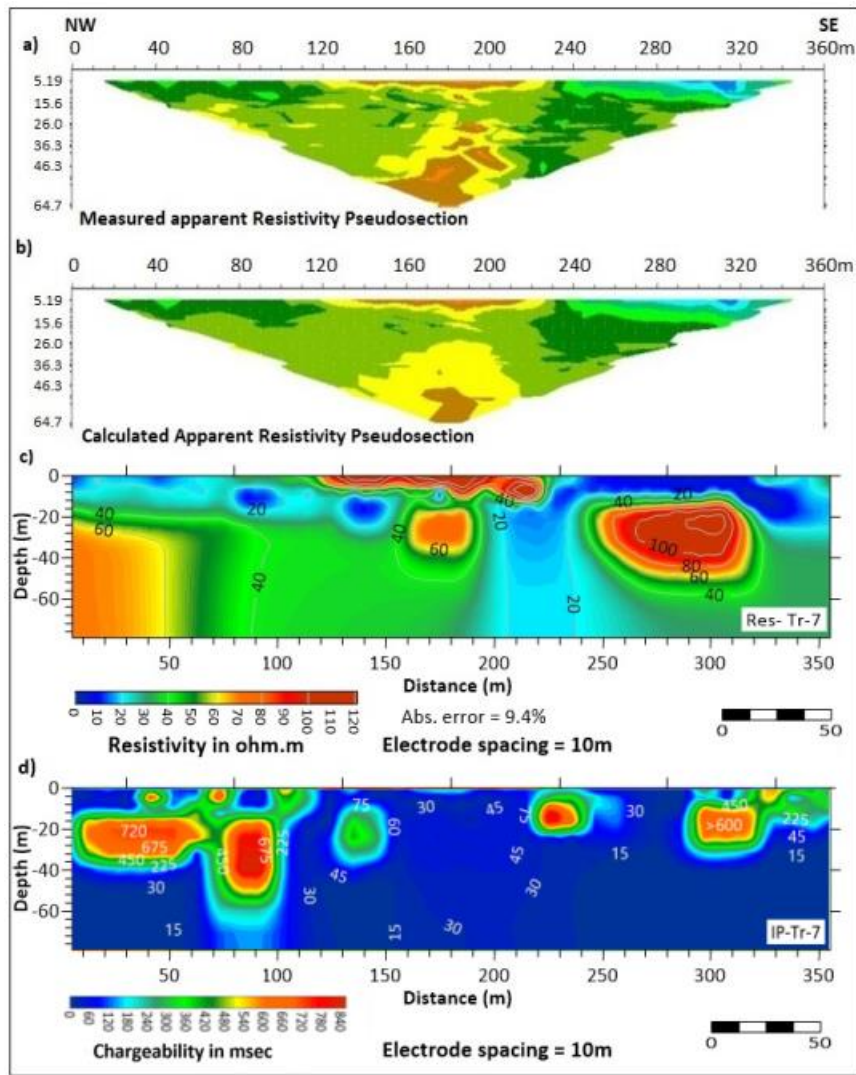


Fig.12. Measured, calculated apparent resistivity pseudosection, ERT inversion model, and IP sections of Tr-7.

The Tr-7 traverse (Fig. 12) has a 360m length and shows the same low and high resistivity features and layers as mentioned in Fig. (11) but it differs in size and shape and is shifted slightly in position too. The strip of low resistivity which represents the first layer is visible here too and at the distance between 200 to 250m. This strip extended downward which might be interpreted as a result of increasing water, clay and silt content. While the high resistivity features ranging from 70 to 100 Ω .m clearly appear on both sides of the traverse with large sizes which may be attributed to the existence of alluvium and gravel deposits with a variable thickness located at top of the section, and at a depth of more than 20m.

The third layer is characterized by a resistivity ranging between 35 to 60 Ω .m associated with the water-saturated marl bed. IP (Fig. 12d) was used as a supporting method of ERT to differentiate between water and clay. In this section at a depth of 0-20m, the low resistivity indicates a medium with mixing low IP, and high IP results. This cleared the ambiguity between clay and water content.

The length of Res-Tr-8 traverse is 400m (Fig. 13). Resistivity distribution of subsurface soil under this traverse shows a strip of low resistivity value ranging between 3 and 15 Ω .m, interpreted to be a first layer consisting of clayey soil. The shallow water level, which appeared on traverse Res-Tr-8 as pockets of low resistivity, may indicate the perched water. Underneath this zone, the resistivity values of second layer range between 20 Ω .m to 80 Ω .m which are corresponding to the marly bed of Tanjero Formation.

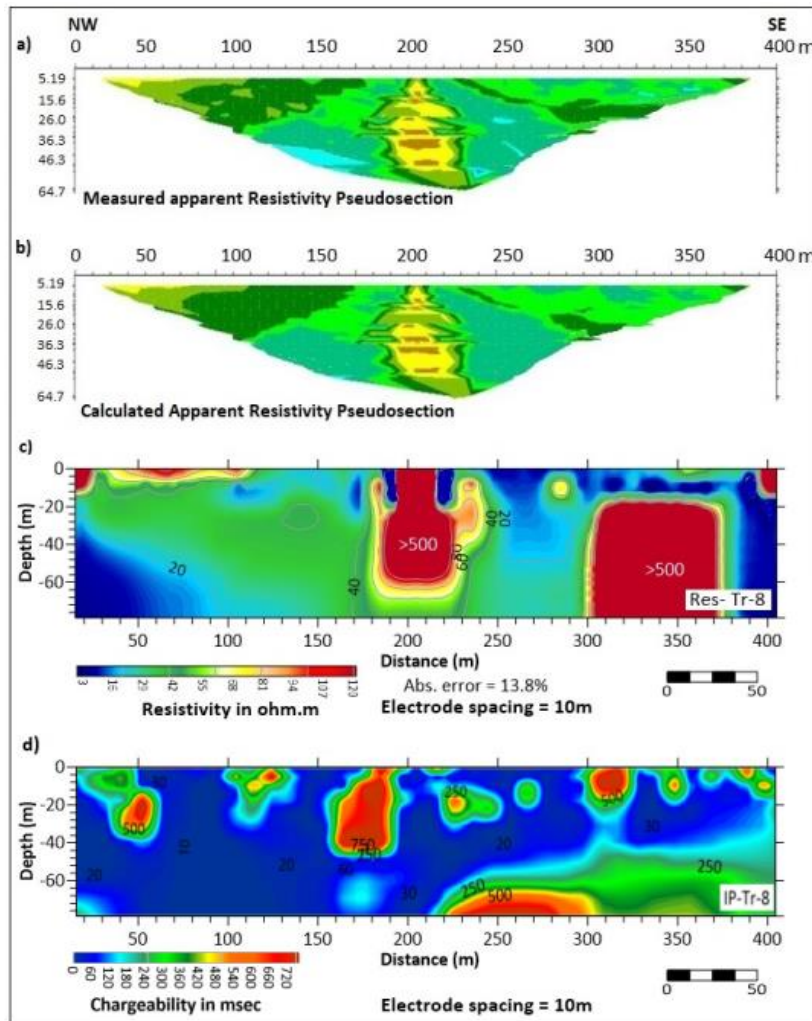


Fig.13. Measured, calculated apparent resistivity pseudosection, ERT inversion model, and IP sections of Tr-8.

The third layer has relatively two high true resistivities (values ranging from 100 to > 500 Ω .m) and vertically elongated shapes. The thickness of the first high resistivity layer is 60m which lies in the central part between a distance of 180-235m, and the second high resistivity layer lies at a depth of 20m near the SE end of the section between a distance of 300 to 320m and extended downward. The near-surface material is due to the presence of boulders exposed on the surface. The broad distribution of resistivity in these sediments is likely influenced by randomness associated with grain size, pore space, and level of water saturation. The pockets of water with low resistivity as mentioned in this traverse are compatible with low IP results. This is shown in the chargeability section (Fig.13d) and the same layer and feature of ERT section are clearly visible in IP section.

The total length of the Res-Tr-9 traverse is 380 m and the depth of investigation reaches 78.8m (Fig. 14). Two zones of low and high resistivities appear on/near the surface that is covered by different lithological components. These sediments are mainly composites of clay and little coarse martial such as fine gravel and pebbly sand (recent sediment). This layer may indicate existence of surface water. The strip of low resistivities zone (from 3 to <30 Ω .m) extended on both sides of the section up to a depth of approximately 20m. In a central upper part, there is a strip of high resistivity value >60 Ω .m observed showing an indication of the presence of coarse material or the presence of a high concentration of water. Underneath this layer is considered a moderate-resistivity value of 40 to 60 Ω .m which might be interpreted as marl and silt content and/or the presence of a high concentration of water (high water-saturated zone). High resistivity features are not visible in this traverse at depths of more than 20m as it appeared in the previous traverses.

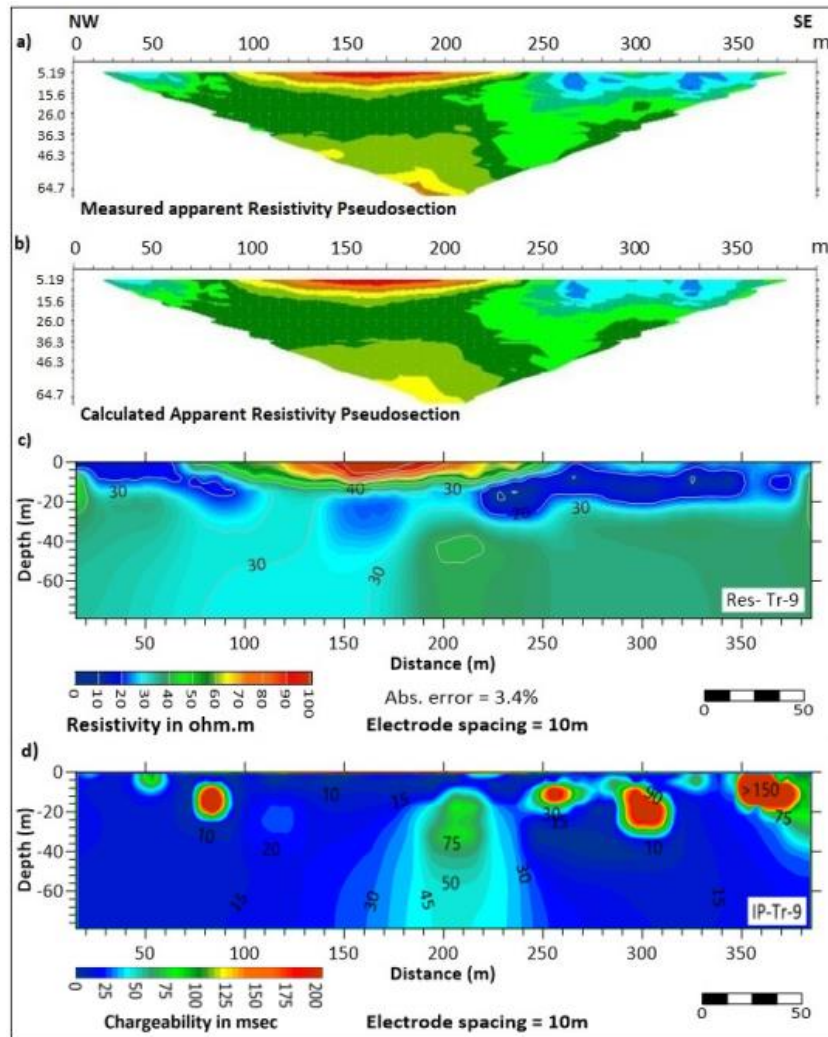


Fig.14. Measured, calculated apparent resistivity pseudosection, ERT inversion model, and IP sections of Tr-9.

Traverse Res-Tr-10 has a length of 390m (Fig. 15) and shows the same main features and layers as indicated in the previous traverse (Res-Tr-7 and 8) with some restrictions. The first layer is represented by a strip of low resistivities (blue color) ranging from $2\Omega.m$ to $20\Omega.s.m$ visible on both sides of the section especially on the NW side. In the second layer, a large high resistivity ($40- > 120\Omega.m$) clearly can be seen at depths of more than 25m at distances between 130 to 210m and extended downward. This feature may be represented due to its composition which contains different types of sediments. The same features have been repeated in traverse Res-Tr-1, 2, and 3. A perched watertable is a kind of phenomenon observed at a depth of approximately 15-30 m. The third layer zone is characterized by a moderate-resistivity value $> 40 \Omega.m$ associated with rarely silt, and marl bed. A water well drilled near the survey line by a distance of about 85m showed a depth of the watertable at 6 m. (Fig. 15d) shows the inversion result of IP giving very high values suggesting that there might be a pipe (or similar metallic feature) beneath the survey line.

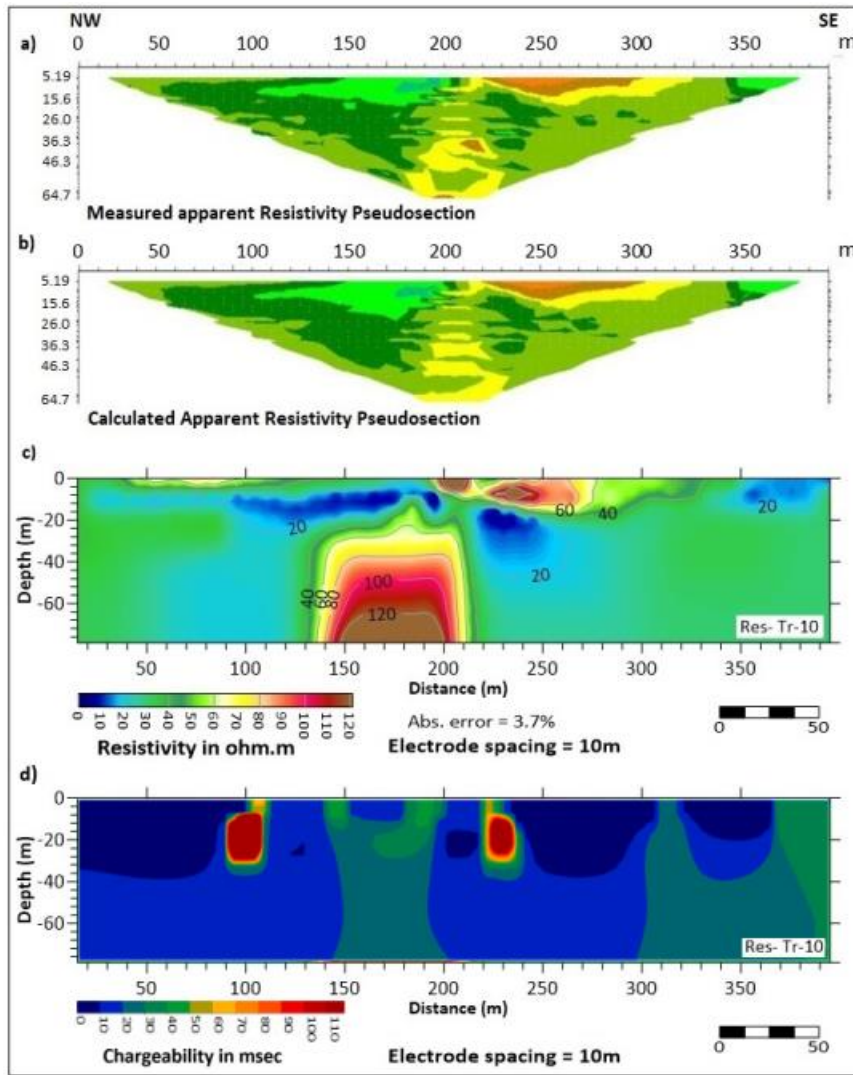


Fig.15. Measured, calculated apparent resistivity pseudosection, ERT inversion model, and IP sections of Tr-10.

Traverse Res-Tr-11 (Fig. 16) was conducted with 400m length. The inverted section shows the same strip of low resistivities near the surface and down to the depths 10-20m while the high resistivity features especially that at the center of the traverse and the other at the SE side of the traverse having $> 50 \Omega.m$. The IP section gives a high value indicating the clay content (Fig. 16d).

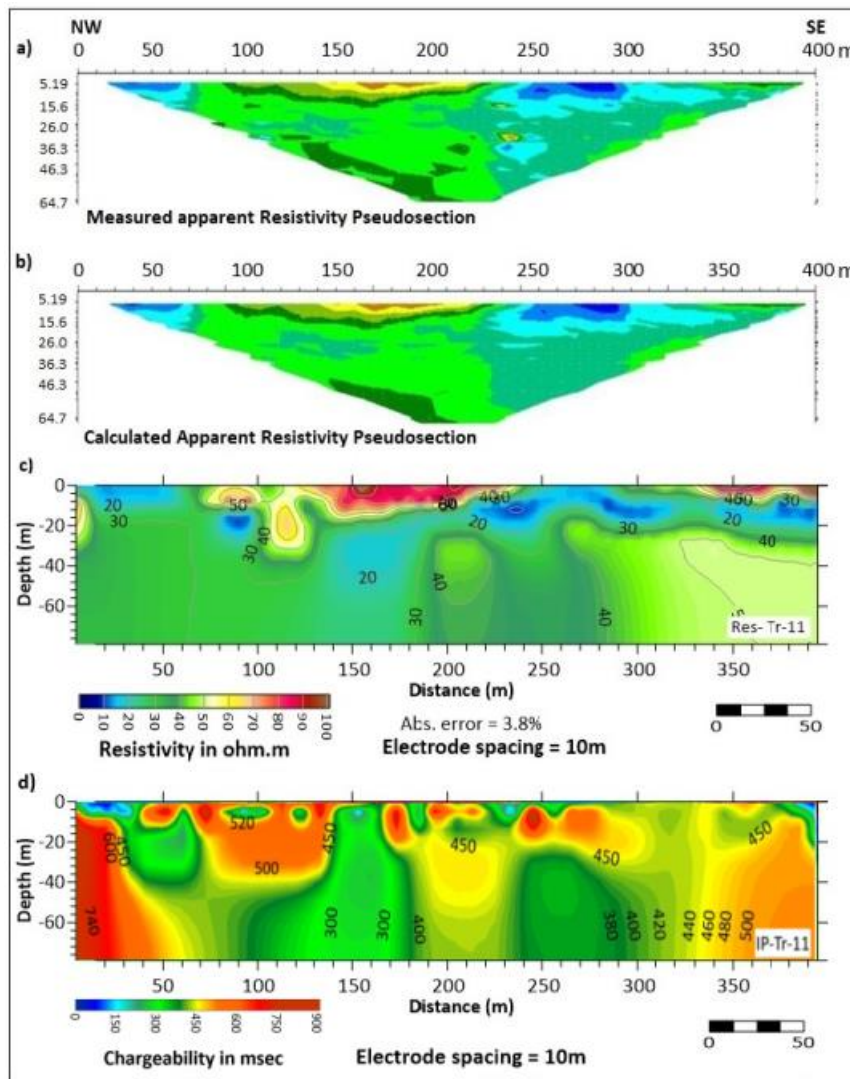


Fig. 16. Measured, calculated apparent resistivity pseudosection, ERT inversion model, and IP sections of Tr-11.

Traverse Res-Tr-12 was conducted also with the same length (400m), and the maximum depth of investigation is 78.8 m (Fig. 17). The resistivity inversion sections show the same features and layers as in Fig. (16) with some differences in size and resistivities amplitude.

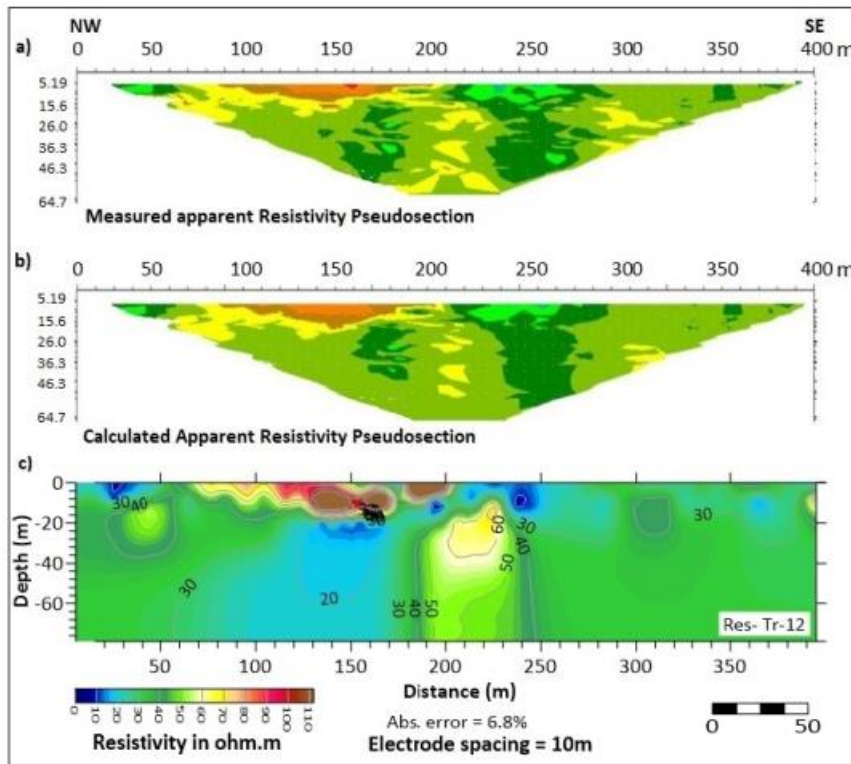


Fig.17. Measured, calculated apparent resistivity pseudosection and ERT inversion model section of Res-Tr-12.

Traverses Res-Tr-13 to, Res-Tr-15, and Res-Tr-18 show the same layers and low and high resistivities features at the same positions with some differences in dimension and resistivity values. Two distinguished low resistivity features circular to oval shapes lie at a distance of 100m and 250m on both sides of the central high resistivity feature that appears on the mentioned traverses. These low resistive layers indicate depressions filled with recent sediments mostly composed of clay with weathered marly of Tanjero Formation. Furthermore, the lateral variation of lithological units can be recognized along this traverse as well as the green layer has a moderate resistivity range (40-60 Ω .m) indicating marl and saturated silt. The central high resistivity feature (concerning other features within the traverses) that lies at a distance between 150 to 220m has sharp vertical sides and seems as a cliff, visible on all the traverses at the same position and approximately the same size. This feature indicates the middle of Tanjero Formation which consists of repetitions of highly fractured marly Limestone interbedded with a layer of sandstone. This layer holds groundwater in some portion (Fig. 18).

Moreover, The Two distinguished low resistivity features appear to be low IP values (Fig. 18d) indicating water content, and in the central part a high resistivity feature is visible in this section.

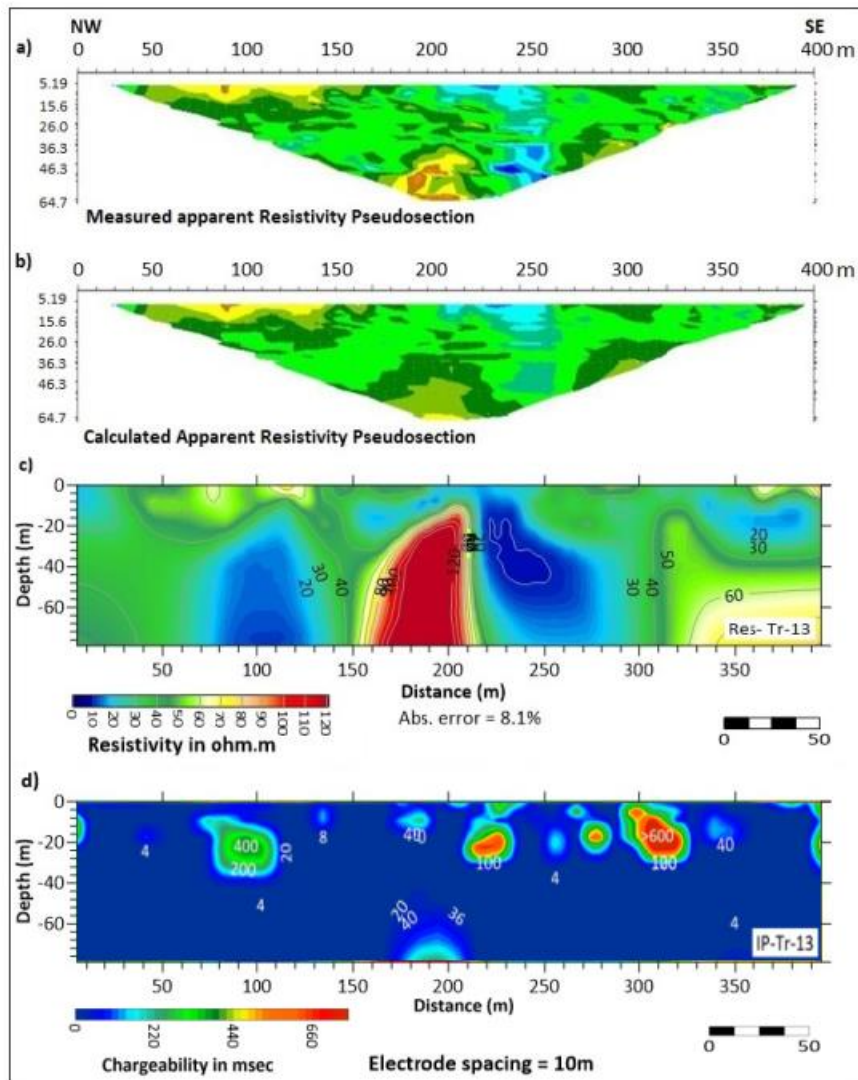


Fig.18. Measured, calculated apparent resistivity pseudosection, ERT inversion model, and IP sections of Tr-13.

Traverse Res-Tr-14 was conducted also with the same length (400m), and the maximum depth of investigation is 78.8 m (Fig. 19). The resistivity inversion sections show the same features and layers as in (Fig.18) with some differences in size and resistivities amplitude. They show resistivity contrast values ranging from 10 to 90 Ω .m in general. The high resistivity subzone layer is restricted to the upper 15 meters of the sections. These high resistivity features probably correspond to the gravel, sand, and silts (rock fragments) with a range of resistivity of 60 to 90 Ω .m which might be the presence of a local aquifer. As well as the second layer with moderate resistivity ranges between 30 to 60 Ω .m which indicates a medium with mixing siltstone, and marl bed. However, the third layer is present at a depth deeper than 7.0 m and all clastic rock layers show resistivity values less than 26 Ω .m. The lateral variation in the resistivity can be noticed clearly in this inversion section. This section in this traverse has almost the same subsurface features as the previous traverse (Res Tr-13) but a different range of resistivity. The IP results (Fig. 19d) are almost the same as the previous traverse (IP-Tr-13).

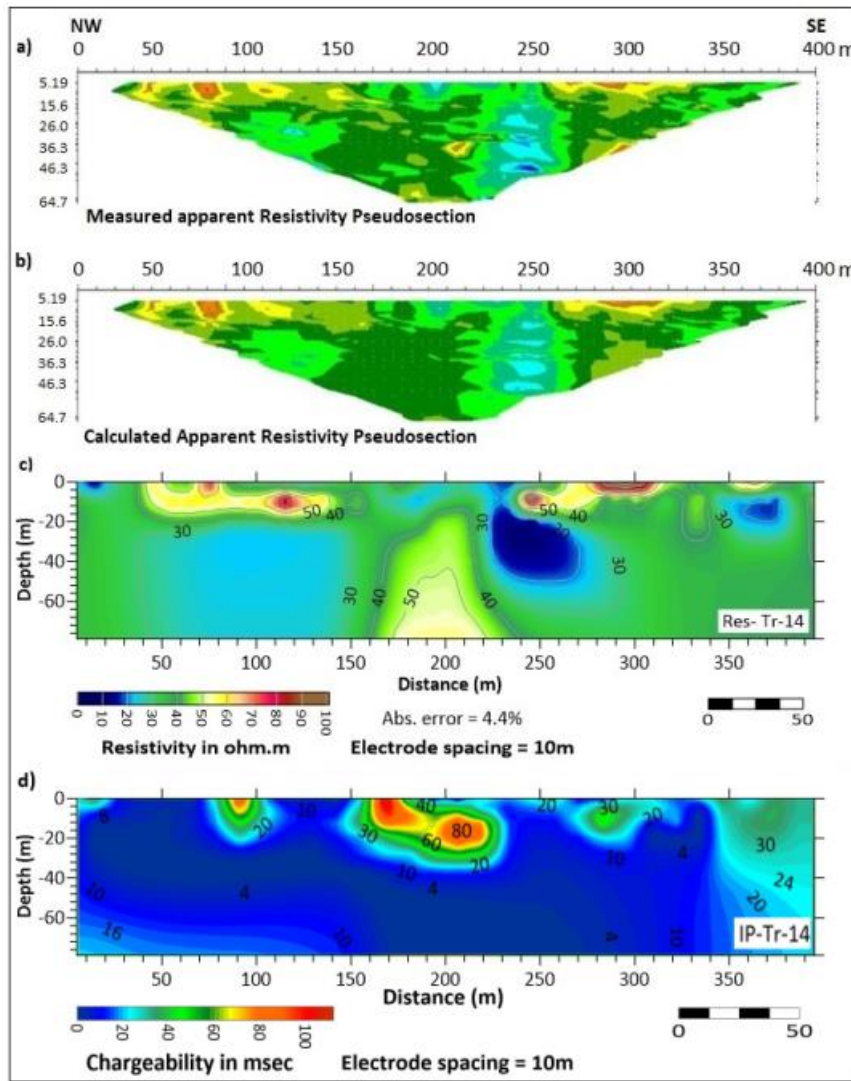


Fig.19. Measured, calculated apparent resistivity pseudosection, ERT inversion model, and IP sections of Tr-14.

Res-Tr-15 traverse is running NW-SE, approximately parallel to the main strike of the outcrops. Three distinguished zones have been identified (Fig. 20). The high resistivity top layer is in the unconsolidated layer range (50-80Ω.m) at a depth of 0-25m which indicated the variation of grain size sediment (sand and gravel bolder). The second layer is characterized by resistivities ranging from 10Ω.m to 30Ω.m, at distances between 40-125 and depths between 25-70m in the left section, and in the right section at distances between 222-270 and depths between 0-68m. This zone is interpreted as depression filled with sediments, and/or the presence of a high concentration of water (high water-saturated zone). Light green to dark green color indicates that the third layer consists of a marl range of resistivity (30-50Ω.m) at depths between 0-78.8m.

According to the above interpretation of the ERT section generally (for low chargeability and low resistivity), the IP value results give more certainty about water content, as shown in Figure 20d.

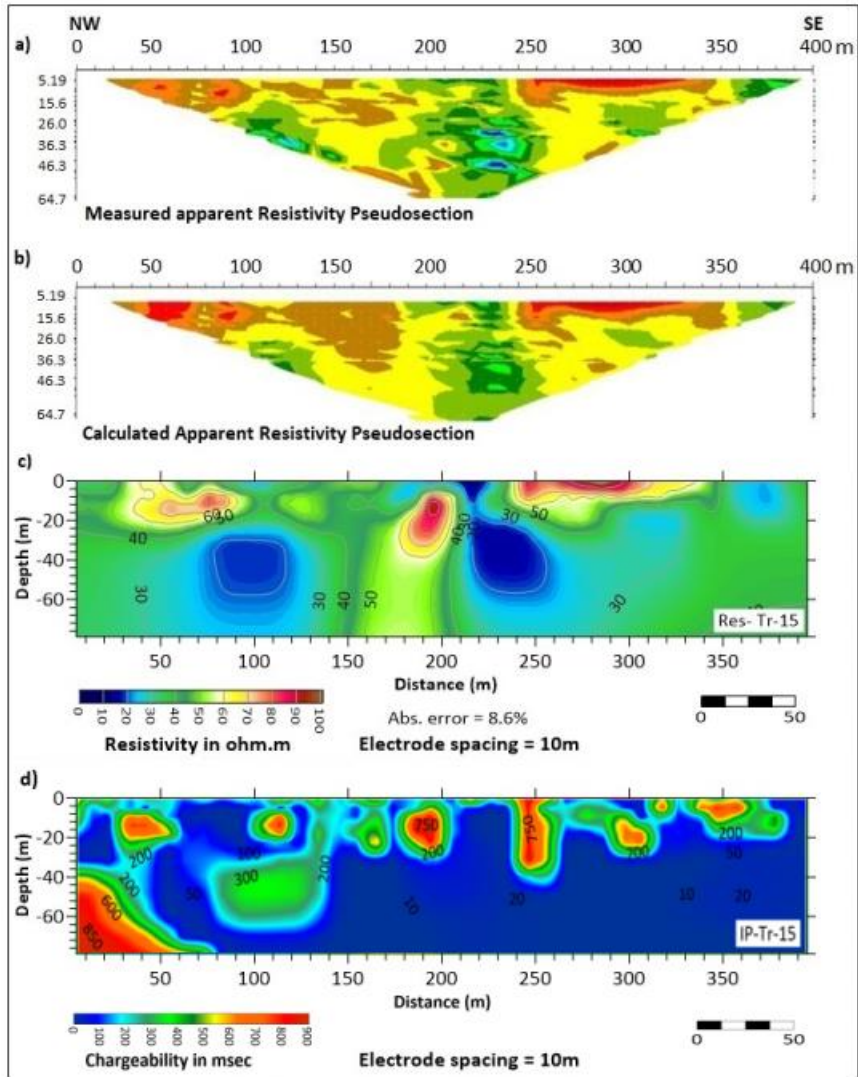


Fig.20. Measured, calculated apparent resistivity pseudosection, ERT inversion model, and IP sections of Tr-15.

The traverse Res-Tr-16 (Fig. 21) consists of a low resistivity (Blue and light blue color) which indicates the presence of groundwater. IP section, the low chargeability and low resistivity cleared the ambiguity to contain clay and water content, except at the near surface of the central part of the traverse where there is a zone of high resistivities that consists of the recent clastic materials (gravel, sand, and silt) and another high resistivity feature appears at a depth of 40 m as it is visible in all other traverses in the same place (Fig. 21d).

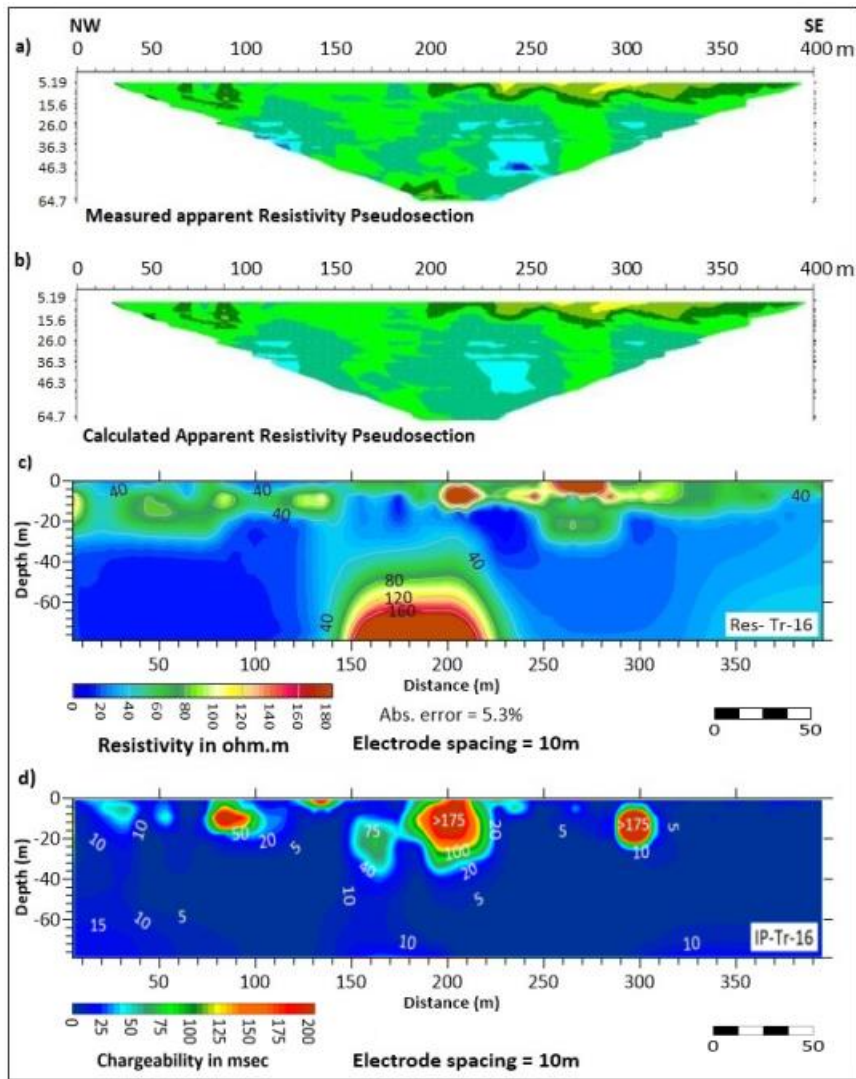


Fig.21. Measured, calculated apparent resistivity pseudosection, ERT inversion model, and IP sections of Tr-16.

The inversion section of the traverse Res-Tr-17 shows a strip of high anomalies appearing as a layer (Fig. 22) of more than 40 to 120 Ω .m consisting of a coarse grain of gravel, sand, and clay. As well as, the horizontal layers in these sections are nearly along the strike of the sediment bedding. While another strip of low resistivities anomalies appearing as a second layer may reflect the presence of groundwater. The central high resistivity also appears with low amplitude and broad shape at the central part of the area too and consists of siltstone and marl bed appearing at a depth of 55m. Generally, the chargeability section (Fig. 22d) shows strong IP (high IP) indicating the presence of the clay layer except several pockets with low IP.

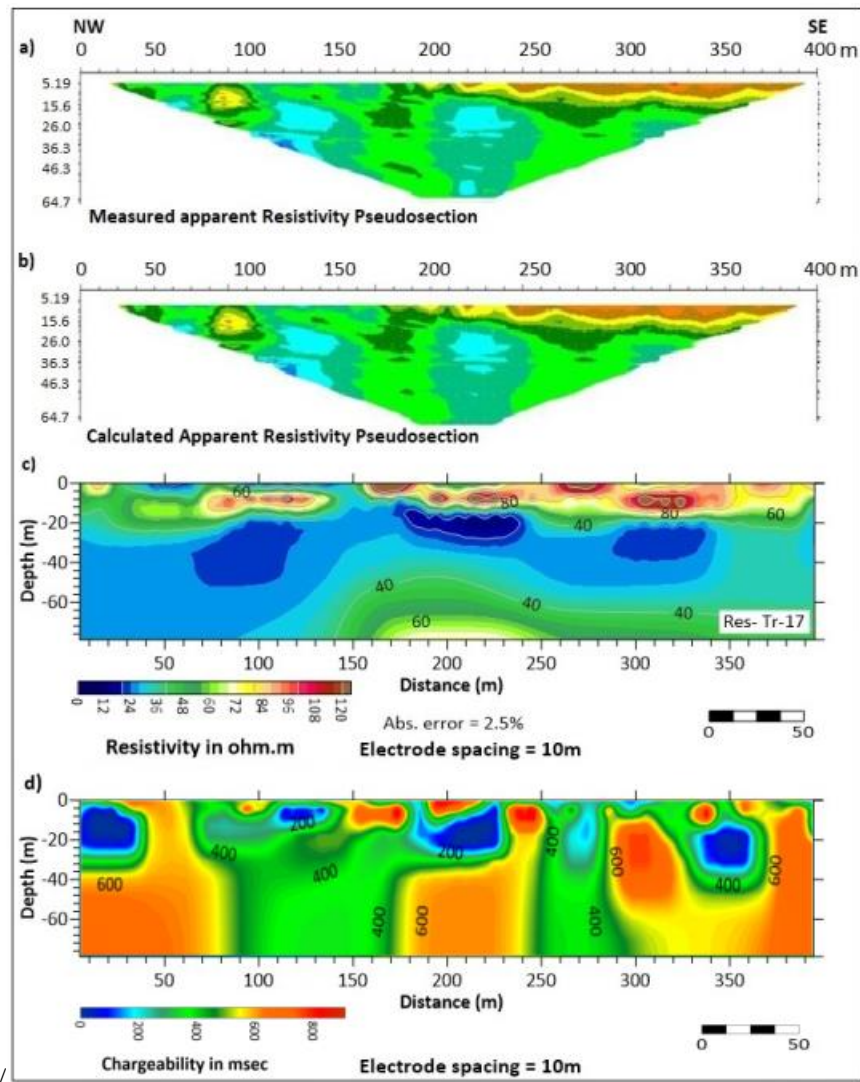


Fig.22. Measured, calculated apparent resistivity pseudosection, ERT inversion model, and IP sections of Tr-17.

In Res-Tr-18 traverse the 2D tomography traverse resistivity inversion results show near-surface lateral variations down to a depth of 20m, and this lateral variation is in the center of the section down to more depth. This layer is covered by a high resistive layer of more than 80 to 100 $\Omega.m$ consisting of coarse grain with mixing clay, fine sand, and gravel, but at down depth it indicates sand or silty organic detrital Limestone of Tanjero formation. At running over beds, the resistivity values are ranging between 5.0 to 20.0 $\Omega.m$ with thicknesses of several meters. which might be interpreted as a result of increasing water and clay content. However, the green color at a depth of deeper than 30m has moderate resistivity which is indicated by the presence of silty marl in Tanjero formation, as shown in a logarithmic scale image (Fig. 23). Approximately at depth 20-40m, the low IP, and low resistivity in this IP section (Fig. 23d) indicate water content.

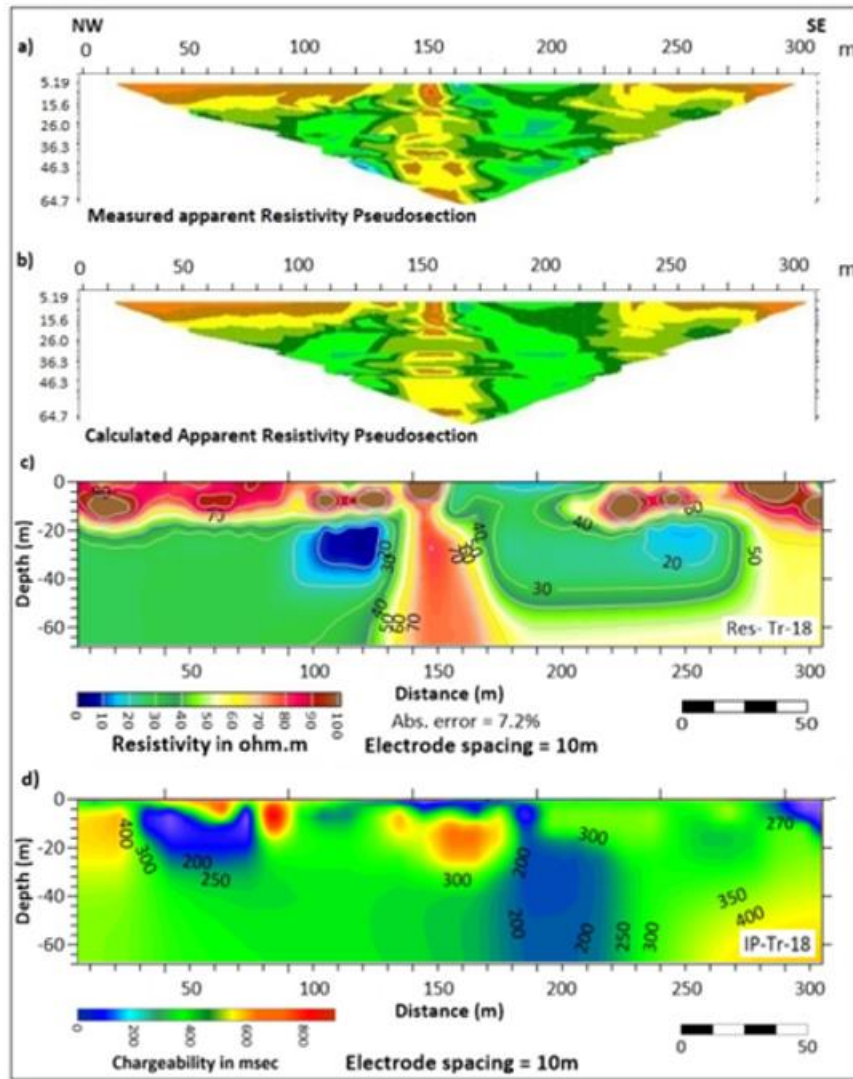


Fig.23. Measured, calculated apparent resistivity pseudosection, ERT inversion model, and IP sections of Tr-18.

Geo-electrical parameters

Hydraulic conductivity and transmissivity are extremely important for the management and development of groundwater resources (Soupios, et al., 2007). Hydraulic conductivity can be considered the basic and main aquifer parameter to estimate the characteristics of the aquifer.

Hydraulic parameters may correlate with the interpreted results of electrical parameters conducted by the Winner- Schlumberger array method of 2D electrical resistivity, through which Dar-Zarrouk parameters including Transverse resistivity (Tr) and longitudinal conductance (SL) can be calculated. The purpose of such correlation is to find out different empirical relationships between these parameters for predicting a more reasonable model that reflects the reliable image of the subsurface aquifer (Frohlic, 1994). The regression technique, utilizing both the resistivity and pumping test data, has been used for the present study to determine the hydraulic properties of the investigated area.

The most important hydraulic parameters concerning aquifers include: -

Porosity (ϕ)

Porosity is defined as the ratio of pore volume saturated with water to the total bulk volume of the rock unit, which is expressed by percentage. Porosity can be determined by many empirical formulas, among these, Archie formula is applied in the current study.

According to the Archie formula, the porosity (ϕ) and Formation factor (F) relationship is given by: -

$$F = a\phi^{-m} \dots\dots\dots (1)$$

$$\phi = (a/F)^{1/m} \dots\dots\dots (2)$$

The resistivity of the water aquifer ρ_w ($\Omega.m$) is determined from the reciprocal of the measured electrical conductivity of the water samples EC ($\mu mols/cm$), which are taken in the wells, distributed throughout the studied area using the following equation:

$$\rho_w = 10000/EC \dots\dots\dots (3)$$

Whereas the resistivity values of the aquifer ρ_r were estimated from the interpretation results. Finally, the aquifer porosities were estimated for the 2D image located at or near the distributed wells of the studied area using the Archie formula in Eq. 2. The constants $a=1$ and m range between 1.3 to 1.6 for unconsolidated sediments (Frohlic, 1974; Kosinski, 1978).

The calculated values of porosity by mentioned formula are formulated in the Table 1. The calculated values of porosity for the aquifer by the Archie's formula range between 32% - 38%. The values of porosity decrease from southwest toward the northeast of the study area.

Table 1. Difference between the calculated aquifer porosity values by the Archie formula at the distributed wells of the studied area.

Wells	wells name	2D Traverse	ρ_r ($\Omega.m$)	EC (mohs / cm)	TDS (ppm.)	ρ_w ($\Omega.m$)	F	m	Porosity by Archie (ϕ)
W1	Shahin city	Res-Tr-15	37	900	576	11.11	3.33	1.1	33
W2	Hawraz Dler	Res-Tr-3	36	850	544	11.76	3.06	1.1	36
W3	Gundi Qularaisi-Sarw	Res-Tr-1	52	750	480	13.33	3.9	1.4	38
W4	Bayza company	Res-Tr-16	57	850	544	11.76	4.85	1.4	32

Transmissivity (T)

Transmissivity is the rate at which groundwater is transmitted through a unit area of an aquifer under a unit hydraulic gradient. It is often expressed as the product of the hydraulic conductivity and the full-saturated thickness of the aquifer and has units of the forms m^3/day .

The purpose of conducting the single well aquifer test, is to calculate the transmissivity by (Cooper and Jacob, 1946) straight-line method for the unconfined aquifer, by applying the manual method (Todd, 1980).

The basic principle of the method is represented by drawing a linear relation on a semi-logarithmic paper between both duration time (t) of the logarithmic scale along the x-axis versus the drawdown (S) along the y-axis (ordinary scale). Then the slope ΔS of the straight line was measured according to this equation: -

$$Slope = 2.3Q/4\pi T \dots\dots\dots (4)$$

Where Q: is water discharge in the well by m^3/day .

In the present study, single well aquifer tests with a short duration of time rate were conducted in 4 wells distributed around the studied area depending on the available data in the Groundwater Directorate of Sulaimani.

The discharge Q for each well was calculated from the results of the pumping tests. Then the transmissivity (T) of the aquifer for each well is calculated using the Cooper-Jacob equation for the unconfined aquifer, as follows: -

$$T=2.3Q/4\pi\Delta S..... (5)$$

Where ΔS: Difference of drawdown per log cycle (1) measured in (m)

The test of data of well No.2 has been taken into account, (Table 2) the data of the single well pumping test (Hawraz well-2), where the Static Water Level (S. W. L) = 27 m, Discharge (Q) = 1.4 Li/sec= 19 Gal/min, Transmissivity (T) = 7.58 m²/day and Hydraulic conductivity (K) = 0.10 m/day.

Table 2. Pumping test data of well No. 2

Time(min)	Drawdown(s)m	Yield (L/Sec)
5	27	---
10	45	4.4
20	58	---
30	66	2.35
45	97	---
60	100	---
90	103	1.8
120	105	---
150	105	1.4

Hydraulic conductivity (K)

Hydraulic conductivity (K) is the rate of movement of water under a unit hydraulic gradient through a porous medium. A more rational concept is permeability. Hydraulic conductivity is the constant of proportionality in Darcy’s Law and as such is defined as the flow volume per unit cross-sectional area of the porous medium under the influence of a unit hydraulic gradient (Alayamani and Sen, 1993). It depends on a variety of physical factors, including porosity, particle size and distribution, shape of particles, arrangement of particles, and other factors (Deming, 2002).

From the manual calculated transmissivity values (T), hydraulic conductivity (K) can be calculated by using the measured saturated thickness of the aquifer (H), which is obtained from a well lithologic, and the calculated value of the 2D-point located at or near the well, by applying the following equation: -

$$T=2.3Q/4\pi\Delta S..... (5)$$

The estimated values of the hydraulic parameters by manual are shown in Table 3. The calculated results of the aquifer transmissivity (T)are ranging between 4.99 -10.6 m²/day. And the calculated results of the hydraulic conductivity (K) are ranging between 0.05-0.17 m/day. Generally, the values ranges of T and K are showing decreasing values from the begging part to end part in the studied area.

Table 3. The results of Transmissivity (T) and hydraulic conductivity (K) calculated by the manual (Cooper and Jacob, 1946) Method.

Well No.	Wells names	2D	Aquifer thickness and resistivity		Darzarrok Parameters		Wells discharge			Hydraulic parameters by the Jaccob method	
			H _{Aq} m.	ρ _{Aq} Ω.m	RT Ω.m ²	SL 1/Ω	Q gal. / min	Q m ³ / day	Slope ΔS/ΔT	T m ² / day	K m/day
W1	Shahin City	T-15	93	37	3441	2.51	15	81.75	3.00	4.99	0.05
W2	Hawraz Dler	T-3	78	36	1188	0.41	19	103.55	2.50	7.58	0.10
W3	Qularaisi-Sarw	T-1	61	52	3172	1.17	16	87.20	1.50	10.65	0.17
W4	Bayza Company	T-16	72	57	4104	1.26	9	49.05	1.50	5.99	0.08

The presence of clay content leads to a decrease in the values of K for the aquifer of the studied area, especially in the direction of southwest toward the northeast of the study area.

Relation between aquifer porosity and resistivity

The relationship between the calculated porosity by Archie formulas is drawn with the resistivity values of the aquifer determined by the interpretation of the 2D points located at or near the location of the wells distributed throughout the studied area, as shown in Fig. 24.

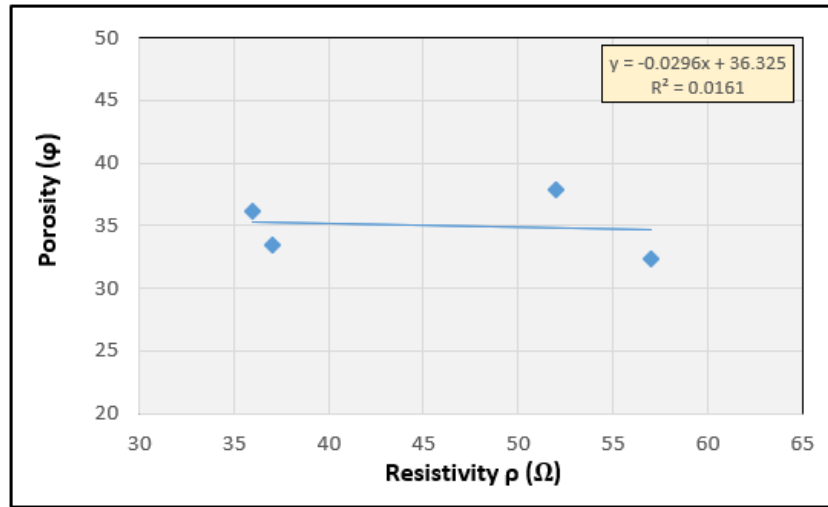


Fig.24. Relations between porosity and aquifer resistivity by applying the Archie formula.

The lower value of the relation coefficient in the case of the Archie formula is another fact which emphasizes the restriction of Archie formula application in the unconsolidated alluvial aquifer of gravel and sand with clay content in the studied area.

Transmissivity (T) and transverse resistivity (ρ_{Tr}) relation

The constructed relation was obtained from pumping test analysis for 4 wells and it revealed a negative relationship with a correlation coefficient ($R^2=0.0669$), as shown in Fig.25.

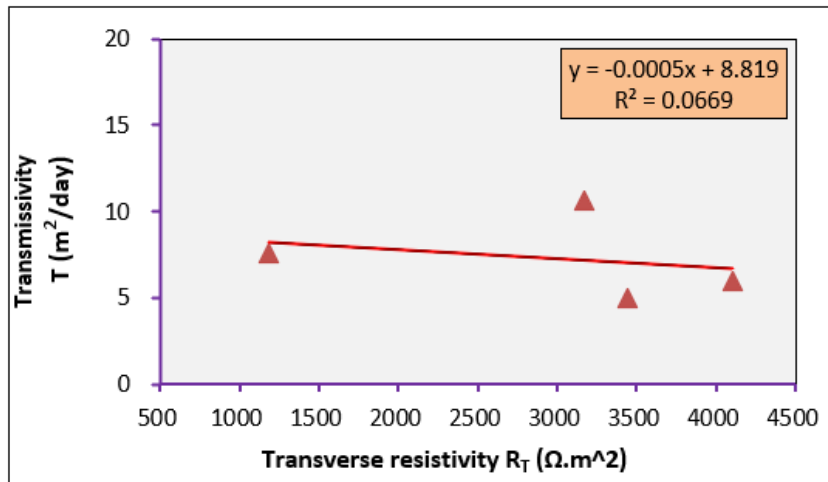


Fig. 25. Relation between transmissivity and transverse resistivity of the aquifer.

The shape of the curve is related to the percentage of clay increase toward the end part of the study. This is the best indication of decreasing gravel sand lithology and porosity.

Hydraulic conductivity with resistivity relations

The relation between hydraulic conductivity (K) and resistivity (ρ) of the aquifer is giving a positive relationship with the relation coefficient ($R^2=0.2091$), as shown in Fig. 26. This result which reflects increasing the porosity providing increase in the hydraulic conductivity especially toward southwestern part of the studied area.

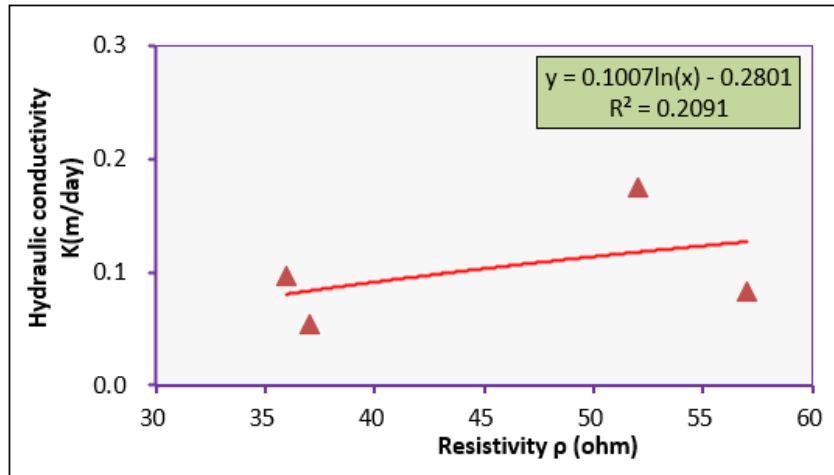


Fig. 26. Relation between hydraulic conductivity and resistivity of the aquifer.

Hydraulic conductivity with transverse resistivity relation

Alternatively, the relation between hydraulic conductivity (K) and transverse resistivity (ρ_{Tr}) is not linear relationship with relation coefficient ($R^2 = 0.03$), as illustrated in Fig. 27.

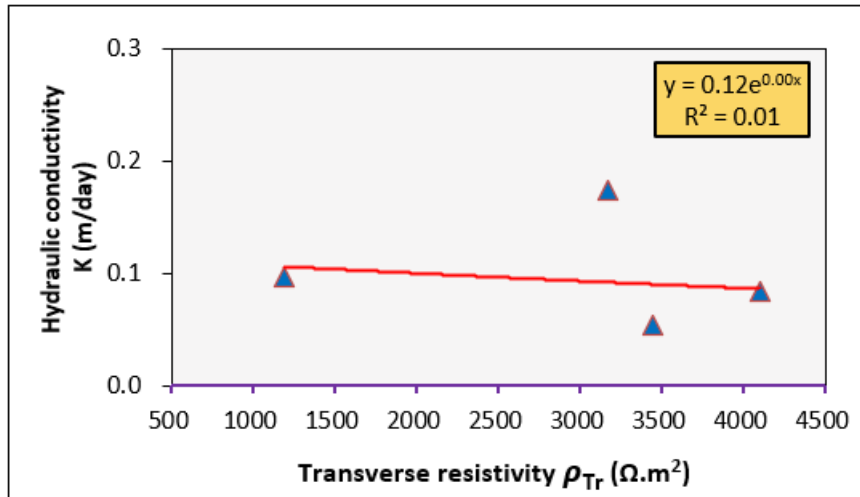


Fig. 27. Relation between hydraulic conductivity and transverse resistivity.

Hydraulic conductivity with longitudinal conductance relation

Another relation between hydraulic conductivity (K) and longitudinal conductance (SL) is also taken, as shown in Fig.28. The relation shows a negative hyperbolic relation with a relation coefficient ($R^2=0.38$).

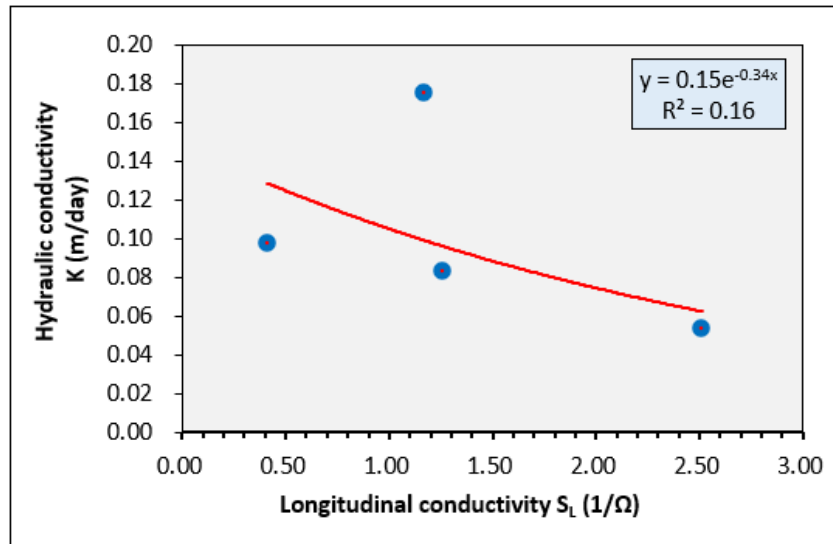


Fig. 28. Relations between hydraulic conductivity and Longitudinal conductivity.

All the above-constructed relationships of hydraulic conductivity (K) and transmissivity (T) with the estimated resistivity (ρ) and Dar Zarrouk aquifer parameters (transverse resistivity (ρ_{Tr}) and longitudinal conductance) are extracted and will clearly show little variations of the hydraulic parameter with the aquifer parameters due to the restriction of the area (small area) under study. The low production of the wells as well as the presence of the clay content, are clearly visible in the porosity relation with aquifer resistivity of the middle Tanjero Fn.

Discussion

The result show that there is variation in all resistivity/IP in the study area. The reason is due to variation in grain size sediment the variation sand, silt, and gravel boulder and the broad distribution of resistivity in these sediments is likely influenced by randomness associated with grain size, pore space, and level of water saturation.

Also presences the most obvious one is a high-resistivity value feature (a dyke shape) that lies at the central part of the section, at depth 20 extended downward having sharp edges at both sides, which may be formed due to the weathering of Tanjero Fn. or probably the mesoscopic structure consisting of different lithology (silty marl and silty organic detrital limestone) and/or the presence of a highly fractured marly Limestone interbedded with a layer of sandstone within Tanjero Fn., this might be interpreted as a result of increasing groundwater and it is formed due to that the area was under the different load of pressure and tectonic stress. Tanjero Fn. crops out within the imbricated and high folded zones in Northeastern Iraq (Karim, 2004). it is visible in all other traverses in the same place.

Furthermore, presences the low resistive layers indicate depressions filled with recent sediments mostly composed of clay with weathered marly of Tanjero Fn. (Fig. 18).

The calculated values of porosity for the aquifer by the Archie formula range between 32% -38%. The values of porosity decrease from southwest toward the northeast of the study area. This is consistent with the result of previous studies conducted with in the same geologic formation (Amin, 2008).

Many relationships of hydraulic conductivity (K) and transmissivity (T) with the estimated resistivity (ρ) Dar Zarrouk aquifer parameters (transverse resistivity (ρ_{Tr}) and longitudinal conductance) were extracted showing little variations of hydraulic parameter with the aquifer parameters due to the restriction of the area (small area) of study little variation in lithology, and the low of the wells production. The presence of the clay content is clearly visible in the porosity relation with aquifer resistivity of the middle Tanjero Fn.

Moreover, the measurements of IP have been extremely successful in distinguishing between clay (with high chargeability and low resistivity) and water (for low chargeability and low resistivity).

Conclusion

In this work, we used an integrated electrical resistivity tomography (ERT) with induced polarization (IP) to remove ambiguity in separating between clay and water content since ERT alone cannot differentiate between clay and water because low resistivity shows either clay or water.

Application of 2D ERT to access influence of geology and lithological formation on groundwater occurrence in the study area was achieved through this study. 2D ERT was used as an effective technique to explain subsurface layers for aquifer characteristics. The aquifer parameters of transmissivity and hydraulic conductivity were calculated from the pump test borehole data and IP technique was also used in the study. Sixteen traverses were collected approximately parallel to the main strike of the outcrops.

The ERT section shows three layers having different electrical properties, the cover thin layer is characterized by a low-resistivity value $< 30 \Omega.m$ which might be interpreted to be increased clay, silt, and water content (high water-saturated zone), with a variable thickness range of 0-20 m. While the second layer has a high range of resistivity (80-120 $\Omega.m$) at depth (range of thickness) >20 m and it is represented a variety of grain size sediment (sand, silt, and gravel). So attention should be taken into consideration in choosing sites for drilling wells. The third layer is considered by a moderate-resistivity value $>50 \Omega.m$ which reflects a bed of marl. Some geological records of the deep wells drilled within this area denote the existence of the Tanjero Formation. We could definitively characterize the high resistivity features that probably correspond to a mesoscopic structure consisting of different lithology (silty marl and silty organic detrital limestone) Within the Tanjero Formation due to the influence of tectonic activity

From all the above-mentioned 2D electrical resistivities, it can be concluded that the resistivity values for the surface layer range between 10 $\Omega.m$ to more than 90 $\Omega.m$. A recent sediment was detected in this area with the thickness range of 1-20m. While for middle Tanjero formation it ranges from more than 60 $\Omega.m$ to less than 100 $\Omega.m$.

The aquifer parameters estimated from the 2D electrical resistivity method for 16 traverses using Dar Zarrouk parameter are in agreement with results obtained from the pump test. The presence of clay content leads to a decrease in the values of hydraulic conductivity (K) and transmissivity (T) for the aquifer of the studied area, especially in the direction of South West toward North East of the study. Increasing the values are due to the presence of sand or gravel.

Acknowledgements

The authors' special thanks go to the staff of Sulaimani Groundwater Directorate especially to Mr. Abbas Ali, the Director of the Directorate, for their assistance and allowing us to borrow (ABEM Terrameter LS) equipment and used it during the fieldwork. Many thanks are due to Dr. Peshawa M., Dr. Twana O. and Mr. Yassin A., for their assistance and supporting us during the preparation of the paper especially during using the ABEM Terrameter LS equipment and providing wells data.

Reference:

- Akhtar, N., Mislan, M.S., Syakir M.I., Anees, M.T. and Yusuf M.S.M., 2021. Characterization of Aquifer System Using Electrical Resistivity Tomography (ERT) and Induced Polarization (IP) Techniques, IOP Conf. Ser.: Earth Environ. Sci. 880 012025, <https://doi:10.1088/1755-1315/880/1/012025>.
- Al-Ansari, N., Ali, A., and Knutsson, S., 2014. Present Conditions and Future Challenges of Water Resources Problems in Iraq. *Water Resource and Protection*, 6(12), pp. 1066-1098.
- Alayamani, M.S. and Sen Z., 1993. Determination of Hydraulic Conductivity from Complete Grain-Size Distribution Curves. <https://www.Connected water.gov.au>.
- Al-Hakari, S.H.S., 2011. Geometric Analysis and Structural Evolution of NW Sulaimani Area, Kurdistan Region, Iraq, Unpublished Ph.D. Thesis, University of Sulaimani, 358 P.
- Ali S.S., 2007. Geology and Hydrogeology of Sharazoor - PIRAMAGROON Basin in Sulaimani Area, Northeastern Iraq, Unpublished Ph.D. Thesis, Faculty of Mining and Geology, University of Belgrade, Serbia, 330 P.
- Al-Manmi, D.A.M., 2002. Chemical and Environmental Study of Groundwater in Sulaymaniyah City and its Outskirts. Unpublished MSc. Thesis, College of Science, University of Baghdad, Baghdad, Iraq, 295 P.
- Al-Qayim, B., 1993. Petrofacies Analysis and Tectonic Evolution of a Zagroside Flysch Suites from Northeastern Iraq. In Kumon and Ku (Eds.), *Petrology of Sandstones in Relation to Tectonics*, V.S.P., Netherlands, pp. 33-42.
- Amin, A.K., 2008. Aquifer Delineation and Evaluation of Hydraulic Parameters from Surficial Resistivity Measurements in Sharazoor Basin, Unpublished Ph.D. Thesis, Dept. of Geology, College of Science, University of Baghdad.
- Aziz N.A., 2012. Three-Dimension Electrical Resistivity and IP Imaging for Soil Layers Investigation at UOT-Baghdad. M.Sc. Thesis.
- Buday, T. and Jassim, S.Z., 1987. The Regional Geology of Iraq: Tectonics, Magmatism, and Metamorphism. In Kassab, I.I. and Abbas, M.J., Eds., *Geology of Iraq*, Geologic Survey, Baghdad, 445 P.
- Cooper, H.H. and Jacob, C.E., 1946. A Generalized Graphical Method for Evaluating Formation Constants and Summarizing Well Field History, *American Geophysical Union Trans.*, Vol. 27, pp. 526-534.
- Dahlin, T., 1996. 2D Resistivity Surveying for Environmental and Engineering Applications. *First Break*, 14, pp. 275-284.
- Deming, D., 2002. *Introduction to Hydrogeology*. McGraw-Hill Higher Education, USA, 468 P.
- Frohlic, R.K., 1974. Combined Geoelectrical and Drill Hole Investigations for Detecting Fresh Water Aquifers in North Western Missouri, *Geophysics*, Vol. 39, No. 3, pp. 340-352.
- Frohlic, R.K., 1994. *Geophysical Method for Hydrogeological and Contaminant (Hydrology Application)*, University of Rhode Island, Water resources research center, 51 P.

- Gao, Q., Shang, Y., Hasan, M., Jin, W., Yang, P., 2018. Evaluation of a Weathered Rock Aquifer Using ERT Method in South Guangdong, China. *Water*, 10, 293.
- Google earth, 2022.
<https://earth.google.com/web/@35.60279421,45.35300994,816.50519849a,1510.42342497d,35y,0.00000003h,0.37944465t,0r>
- Haeni F.B., 1988. Application of Seismic Refraction Technique to Hydrologic Studies, United States Government Printing Office, Washington, 95 P.
- Hasan, M., Shang, Y., Jin, W., Akhter, G., 2020. An Engineering Site Investigation Using Non-Invasive Geophysical Approach. *Environ. Earth Sci.*, 79, 265.
- Jackson, P.N., Taylor, S.D., and Stanford, P.N., 1978. Resistivity-Porosity-Particle Shape Relationships for Marine Sands, *Geophysics*, 43, pp. 1250-1268.
- Johnson, T.C., Versteeg, R.J., Ward, A.F., Day-Lewis, D., Revil, A., 2010. Improved Hydrogeophysical Characterization and Monitoring Through High Performance Electrical Geophysical Modeling and Inversion. *Geophysics*, 75, WA27–WA41.
- Karim H, AL-Qaissy M, Aziz N.A., 2014. 2D and 3D Resistivity Imaging for Soil Site Investigation. *Eng Tech J* 32:249–272.
- Karim, K.H. and Khanaqa, P., 2017. Stratigraphy and Structure of the Southeastern Part of Piramagrun Anticline, Sulaimani Area, Northeast Iraq. *Bulletin of the Mineral Research and Exploration Journal*, Vol.154, pp. 27-39, <https://doi:10.19076/mta.288708>.
- Karim, K. H., (2004). Basin analysis of Tanjero Formation in Sulaimaniya area, NE-Iraq. Unpublished PhD thesis, University of Sulaimani, 133 P.
- Kosinsiki, W.K., 1978. Geoelectrical Studies for Predicting Aquifer Properties. M.Sc. Thesis, University of Rhode Island, USA.
- Loke, M.H., 2017. Geoelectrical Imaging 2-D and 3-D. GEOTOMOSOFT SOLUTIONS. Manual books.
- Loperte, A., Soldovieri, F., Palombo, A., Santini, F., Llapenna, V., 2016. An Integrated Geophysical Approach for Water Infiltration Detection And Characterization at Monte Cotugno Rock-Fill Dam (Southern Italy). *Eng. Geol.*, 211, pp. 162–170.
- Ma’ala, K.A., 2008. Geological Map of the Sulaimaniyah Quadrangle, Sheet N1-38-3, Scale 1:20000, GEOSURV, Baghdad.
- Mota, L., 1954. Determination of Dips and Depths of Geological Layers by the Seismic Refraction Method, *Geophysics*, Vol. 19, pp. 242-254.
- Payal R., 2017. Geophysical Modeling for Groundwater and Soil Contamination Risk Assessment, Ph.D. Thesis, Università Degli Studi Di Napoli Federico II.
- Revil, A., Murugesu, M., Prasad, M., Le Breton, M., 2017. Alteration of Volcanic Rocks: A New Non-Intrusive Indicator Based on Induced Polarization Measurements. *J. Volcanol. Geotherm. Res.*, 341, pp. 351–362.
- Samyn, K., Mathieu, F., Bitri, A., Nachbaur, A., Closset, L., 2014. Integrated Geophysical Approach in Assessing Karst Presence and Sinkhole Susceptibility Along Flood-Protection Dykes of the Loire River, Orléans, France. *Eng. Geol.*, 183, pp. 170–184.
- Sarntima, T., Arjwech, R., Everett, E.M., 2019. Geophysical Mapping of Shallow Rock Salt at Borabue, Northeast Thailand, Near Surface Geophys 17, pp. 403–416, <https://doi:10.1002/nsg.12052>.
- Sharbazheri, K., Ghafor, I., Muhammed, Q., 2009. Biostratigraphy of the Cretaceous/Tertiary Boundary in the Sirwan Valley, Sulaimani Region, Kurdistan, NE Iraq. *Geol. Carpathica* 2009, 60, pp. 381-396.

- Sissakian, V.K. and Fouad, S.F., 2015. Geological Map of Sulaimaniyah Quadrangle, at Scale of 1: 250 000, Journal of Zankoi Sulaimani, Part-A- (Pure and Applied Sciences).
- Slater, L. and Lesmes, D., 2002. IP Interpretation in Environmental Investigations. Geophys., 67, pp. 77-88.
- Slater, L. and Sandberg, S., 2000. Resistivity and Induced Polarization Monitoring of Salt Transport Under Natural Hydraulic Gradients. Geophys., 65, pp. 408-420.
- Soupios, P.M., Kouli, M., Valliantos, F., Vafidis, A., Stavroulakis, G., 2007. Estimation of Aquifer Hydraulic Parameters from Surficial Geophysical Methods: A Case Study of Keritis Basin in Chania (Crete- Greece). J. Hydrol., 338, pp. 122–131.
- Stevanovic, Z., and Markovic, M., 2003. Hydrogeology of Northern Iraq, Climate, Hydrology, Geomorphology and Geology, Vol.1, 2nd Edition, FAO.
- Todd, D.K., 1980. Groundwater Hydrology, Second Edition, Consulting Engineering INC. Jhon Wiley and Sons, New York, USA, 535 P.
- Zohdy, A.A.R., 1969. Application of Deep Electrical Sounding for Groundwater Exploration in Hawaii, Geophysics, 34, pp. 584-600.